NATIONAL ADVISORY COMMITTEE FOR AERONAUTICS

TECHNICAL NOTE

No. 1367

EFFECT OF EXHAUST PRESSURE ON THE PERFORMANCE OF A 12-CYLINDER LIQUID-COOLED ENGINE

By Leland G. Desmon and Ronald B. Doyle

Flight Propulsion Research Laboratory
Cleveland, Ohio

Washington
July 1947

NATIONAL ADVISORY COMMITTEE FOR AERONAUTICS

TECHNICAL NOTE NO. 1367

EFFECT OF EXHAUST PRESSURE ON THE PERFORMANCE OF A 12-CYLINDER LIQUID-COOLED ENGINE

By Leland G. Desmon and Ronald B. Doyle

SUMMARY

A dynamometer-stand investigation was conducted to determine the effect of exhaust pressure on the performance of a 12-cylinder liquid-cooled aircraft engine equipped with a conventional exhaust collector. The investigation covered a range of exhaust pressures from about 7 to approximately 62 inches of mercury absolute, engine speeds from 1600 to 3000 rpm, inlet-manifold pressures from 30 to 50 inches of mercury absolute and fuel-air ratios of 0.063, 0.069, 0.085, and 0.100.

The results are presented in the form of curves that show the effect of exhaust pressure on engine power, charge-air flow, volumetric efficiency, inlet-manifold mixture temperature, exhaust-gas temperature, cylinder-head temperature, and heat rejected to the coolant.

INTRODUCTION

As a part of the general study of composite-engine performance, dynamometer-stand investigations are being conducted at the NACA Cleveland laboratory to determine the effect of exhaust pressure on the performance of several aircraft engines.

An analysis of this effect and a method of data presentation are developed in reference 1. The results of investigations of the effect of exhaust pressure on engine performance conducted on two different models of an 18-cylinder, air-cooled, radial engine are presented in references 2 and 3.

Reported herein are the results of an investigation, similar to those of references 2 and 3, conducted on a liquid-cooled aircraft engine over a range of exhaust pressures for various engine speeds, inlet-manifold pressures, and fuel-air ratios. The effect of exhaust pressure on engine power, charge-air flow, volumetric

efficiency, inlet-manifold mixture temperature, exhaust-gas temperature, cylinder-head temperature, and heat rejected to the coolant is presented in the form of generalized curves.

INSTALLATION AND INSTRUMENTATION

Pertinent specifications of the 12-cylinder V-1710 engine used in the investigation are:

Bore, inches	5.50
Stroke, inches	6.00
Displacement, cubic inches	1710
Compression ratio	6.65
Propeller-reduction-gear ratio	2:1
Valve timing	
Inlet opens, degrees B.T.C.	48
Inlet closes, degrees A.B.C.	62
Exhaust opens, degrees B.B.C.	76
Exhaust closes, degrees A.T.C.	26
Valve overlap, degrees	74
Supercharger impeller diameter, inches	9.5
Supercharger-gear ratio	8.1:1
Spark advance, degrees B.T.C.	
Inlet side	28
Exhaust side	34

A general view of the engine installation is shown in figure 1; a schematic diagram of the combustion-air, engine-oil, and coolant systems is presented in figure 2. The engine was connected by an extension shaft and two flexible couplings to a 2000-horsepower eddy-current dynamometer. Dynamometer torque was measured with a balanced-diaphragm torquemeter of the type described in reference 4. Engine speed was measured with a chronometric tachometer.

Part of the program was conducted with the engine drawing the charge air from the room. When the desired inlet-manifold pressure was unattainable in this way, the laboratory combustion-air system was used to increase the pressure at the carburetor inlet. A butterfly valve, located in the charge-air intake pipe between the air-measuring orifice and the engine, was used to adjust the carburetor-inlet pressure. The brake horsepower presented is therefore the power determined from the dynamometer with no deduction for the supercharger work required to provide the above-atmospheric carburetor-inlet pressures.

A thin-plate orifice, installed according to A.S.M.E. specifications, was used for measuring the charge-air flow. The

carburetor-inlet pressure was measured at the standard carburetor impact tap and the inlet-manifold pressure was measured at the right rear branch of the inlet manifold. Pressures were also measured in the other branches of the inlet manifold; the right rear branch pressure was within one-half percent of the average for the range of test conditions. The carburetor-inlet air temperature was measured by means of four iron-constantan thermocouples connected in parallel and mounted $3\frac{1}{2}$ inches above the carburetor top deck. Four iron-constantan thermocouples, one in the priming tap in each three-cylinder branch of the inlet manifold (as seen in fig. 3), were connected in parallel to measure the inlet-manifold mixture temperature.

The investigation was conducted with fuel conforming to AN-F-28, Amendment-2; the fuel flow was measured with a calibrated rotameter. In conjunction with the standard carburetor mixture control used for coarse regulation of fuel flow, a needle valve in a line connecting the high-pressure fuel chamber of the carburetor with the fuel-injection nozzle and a needle valve in an air bleed line connecting the air chambers of the carburetor were used to make small adjustments in fuel flow.

The exhaust-gas collector was the type used on the P-38 airplane modified to incorporate bellows-type expansion joints to insure a gastight system. A sketch of the engine exhaust system is shown in figure 3. The collector was attached to the laboratory altitude exhaust system through a length of 8-inch diameter pipe. Engine exhaust pressure was controlled by throttling the gas with a butterfly valve in the laboratory exhaust system. A piezometer ring, located approximately 1 foot downstream of the junction of the two collector halves, was used in measuring the engine exhaust pressure. Exhaust-gas temperatures were measured about 8 inches downstream of the piezometer ring with three quadruple-shielded chromel-alumel thermocouples located on one circumference and spaced 120°; the depth of immersion was approximately one-third of the exhaust-duct diameter. The average of the temperatures indicated by the three thermocouples was taken as the exhaust-gas temperature.

The engine coolant system was pressurized by conducting regulated compressed air to the coolant expansion tank. A steam heater, a water-cooled heat exchanger, and an automatically operated mixing valve provided a constant engine-coolant outlet temperature. An auxiliary pump and a throttle valve were used to regulate the flow and the coolant pressure on the inlet side of the engine pump.

A thin-plate orifice installed according to A.S.M.E. specifications was used in measuring the coolant flow during the runs at inlet-manifold pressures of 40 and 50 inches of mercury absolute. Coolant data were not obtained during the runs made at an inlet-manifold pressure of 30 inches of mercury absolute. Copper-constantan thermocouples were located at the coolant inlet and outlet in each cylinder bank. Coolant temperatures were read with the aid of a spotlight galvanometer and a manual balancing potentiometer to obtain accuracy.

A nominal 70-30 (by volume) ethylene glycol-water mixture was used as the engine coolant and its actual composition was checked during the investigation by determining its boiling point.

The average cylinder-head temperature was obtained with 12 iron-constantan thermocouples, one embedded between each pair of exhaust valves.

A magnetic-vibration type detonation pickup was installed at each of the exhaust spark plugs for runs made at inlet-manifold pressures of 40 and 50 inches of mercury absolute and detonation signals were indicated on a cathode-ray oscillograph.

All pressures were read on manometers and, with the exception of the coolant temperature rise, all temperatures were indicated on self-balancing type potentiometers.

PROCEDURE

The dynamometer-stand investigation was conducted over a range of exhaust pressures from about 7 to approximately 62 inches of mercury absolute for ranges of engine speeds from 1600 to 3000 rpm, inlet-manifold pressures from 30 to 50 inches of mercury absolute, and fuel-air ratios from 0.063 to 0.100. All runs were made with the engine throttle full open.

At low fuel-air ratios and certain engine speeds, the exhaust-pressure range over which data could be obtained was initially limited by engine surge. This surge was traced to an unstable fuel-enrichment valve in the injection-type carburetor and the condition was remedied sufficiently to permit operation over a large portion of the exhaust-pressure range.

The engine operating conditions at which runs were made and the conditions at which incipient detonation and engine surging were encountered are given in table I. The engine was not run in the detonation range.

The carburetor-air temperature was 550 ± 15° R; the oil-inlet temperature was maintained at 150 ± 5° F by automatic control; the coolant-out temperature was held constant at 220 ± 5° F. For each of the 40- and 50-inch inlet-manifold pressure runs, the measured coolant flow was 0.710 ± 0.001 pound per engine revolution or about 250 gallons per minute at an engine speed of 3000 rpm. Sufficient time was allowed at each exhaust pressure for the cylinder-head and coolant temperatures to reach equilibrium before data were taken.

SYMBOLS

The following symbols are used in the calculations:

c	specific heat of coolant, (Btu)/(lb)(°F)
f	fuel-air ratio
fhp	mechanical friction horsepower
g	acceleration due to gravity, 32.2 (ft)/(sec)^2
H	heat rejected to coolant, (Btu)/(min)
ihp	indicated horsepower of engine
imep	indicated mean effective pressure, (lb)/(sq ft)
N	engine speed, (rpm)
php	pumping horsepower
p_e	engine exhaust pressure, (lb)/(sq ft absolute)
p_m	inlet-manifold pressure, (lb)/(sq ft absolute)
q/η	ratio of pressure coefficient to adiabatic supercharger efficiency (assumed to be 1.0)
R	gas constant for air, (ft-lb)/(lb)(°F)
shp	engine-stage supercharger horsepower

T_m measured inlet-manifold mixture temperature, (°R)

t_1 coolant inlet temperature, (°F)

t_2 coolant outlet temperature, (°F)

U supercharger impeller tip speed, (ft)/(sec)

v_d displacement volume of engine, (cu ft)

W_c measured charge-air flow, (lb)/(sec)

W_l coolant flow, (lb)/(min)

η_g supercharger-drive gear efficiency (assumed to be 0.85)

η_v volumetric efficiency

ϕ ratio of indicated mean effective pressure to inlet-manifold pressure, $\frac{imep}{p_m}$

METHODS OF CALCULATION

Effect of exhaust pressure on indicated power. - The effect of exhaust pressure on indicated power is correlated by plotting the dimensionless quantity ϕ (ratio of the indicated mean effective pressure to the inlet-manifold pressure) against p_e/p_m (ratio of engine exhaust pressure to inlet-manifold pressure). As in reference 2, the quantity ϕ was computed from the data by the relation

$$\phi = \frac{imep}{p_m} = \frac{2 \times 33{,}000\ ihp}{p_m\ v_d\ N} \qquad (1)$$

The indicated horsepower, which is defined to include the contributions of all four strokes of the cycle, is taken as the sum of the brake, the engine-stage supercharger, and the mechanical friction horsepowers.

Engine-stage supercharger horsepower shp was obtained by the relation

$$shp = \frac{W_c\ (1 + f)\ U^2}{550\ g\ \eta_g}\ \frac{q}{\eta} \tag{2}$$

Mechanical friction horsepower fhp was computed from the equation

$$fhp = kN^2 \tag{3}$$

where k is a constant equal to 1.9602×10^{-5}. The value of k, corresponding to the bore, the stroke, and the number of cylinders of the engine, was determined from an empirical relation based on a large amount of data obtained on various types of reciprocating engine. Friction horsepower thus determined is due only to rubbing and includes no pumping power. Except where otherwise noted, the indicated horsepower (and hence ϕ) was corrected to a constant inlet-manifold mixture temperature of 660° R on the assumption that indicated horsepower varied inversely as the absolute inlet-manifold mixture temperature.

Effect of exhaust pressure on brake horsepower. - The effect of exhaust pressure on brake horsepower is presented in plots of brake horsepower against p_e/p_m.

Brake horsepower was corrected to a carburetor-air temperature of 550° R assuming it varied inversely as the square root of the absolute temperature.

Volumetric efficiency. - Volumetric efficiency η_v is defined as the ratio of the volume of charge air taken into the engine per cycle at the pressure and the temperature in the inlet manifold to the displacement volume of the engine and is calculated from the expression

$$\eta_v = \frac{2 \times 60\ R\ T_m\ W_c}{p_m\ v_d\ N} \tag{4}$$

Variation of horsepower with charge-air flow. - Inasmuch as the power obtained during the compression and expansion strokes is approximately proportional to the charge air in the cylinder at the instant of valve closure for a given engine, spark setting, and fuel-air ratio, plots of this power against charge-air flow were made to show the accuracy of the data. An estimate of this power (the indicated horsepower of the intake and exhaust strokes) was obtained by subtracting the pumping horsepower php from indicated horsepower ihp. Pumping horsepower was calculated as follows assuming a square indicator card for the intake and exhaust strokes:

$$\text{php} = \frac{(p_m - p_e)\, v_d\, N}{2 \times 33{,}000} \tag{5}$$

The quantity (ihp - php) is plotted against charge-air flow. Both terms were corrected to an inlet-manifold mixture temperature of 660° R.

Heat rejected to coolant. - The heat rejected to the coolant was calculated from the temperature rise, the coolant flow, and the specific heat by the expression

$$H = c(t_2 - t_1)\, W_l \tag{6}$$

In making the computations, corrections were made for variations in the specific heat of the coolant with temperature and coolant composition. The values of the specific heat of the ethylene glycol and water mixture were obtained from reference 5.

RESULTS AND DISCUSSION

Effect of exhaust pressure on indicated horsepower. - The variation of ϕ with p_e/p_m for constant engine speeds, inlet-manifold pressures, and fuel-air ratios is shown in figure 4. The plots are keyed for inlet-manifold pressure. Inasmuch as ϕ in this figure was corrected to a constant inlet-manifold mixture temperature, it does not include the effect of increasing inlet-manifold mixture temperature, which, in actual operation at constant carburetor temperatures (as discussed later), was found to accompany increasing exhaust pressure.

Inspection of figure 4 shows that, for constant engine speed and fuel-air ratio, ϕ is nearly independent of inlet-manifold pressure for the range covered; ϕ decreases as p_e/p_m increases. Comparison of the curves at constant fuel-air ratios and p_e/p_m

shows that ϕ has a maximum value near an engine speed of 2400 rpm. In general, a comparison at constant engine speed and p_e/p_m shows that, for those fuel-air ratios investigated, ϕ has a maximum value at a fuel-air ratio of 0.085.

Effect of exhaust pressure on brake horsepower. - The variation of engine brake horsepower with p_e/p_m for constant engine speeds, inlet-manifold pressures, and fuel-air ratios is shown in figure 5. Although these curves include the effect of varying inlet-manifold mixture temperature (because brake horsepower was corrected to a constant carburetor-air temperature), they are of the same general shape as those of figure 4. These temperature effects will be discussed in conjunction with subsequent curves. In order to facilitate the evaluation of the carburetor-inlet pressure corresponding to the various conditions, the variation of the ratio of inlet-manifold pressure to full-throttle carburetor pressure p_m/p_c with engine speed is shown in figure 6. The curve, which is plotted for a nominal carburetor-inlet temperature of 550° R, is estimated to be accurate within $\pm 1\frac{1}{2}$ percent for all engine conditions investigated. Many of the data points are coincident and only the faired curve is shown.

The values of p_m/p_c in figure 6 with the values of the charge-air flow obtainable from subsequent figures permit the computation of the auxiliary supercharger power required to provide the desired carburetor-air pressure at a given altitude. This auxiliary supercharger power should be subtracted from the values of bhp reported. For some runs the desired carburetor pressure was unobtainable except with the aid of the laboratory air supply.

Effect of exhaust pressure on charge-air flow and volumetric efficiency. - The variation of charge-air flow, corrected to a carburetor-air temperature of 550° R, with p_e/p_m for constant engine speeds, inlet-manifold pressures, and fuel-air ratios is shown in figure 7. Figure 8 shows the variation of volumetric efficiency η_v with p_e/p_m for the same range of engine conditions.

The curves in figures 7 and 8 have the same general shape as the power curves. The plots of volumetric efficiency are independent of inlet-manifold pressure and are only slightly affected by fuel-air ratio.

Variation of horsepower with charge-air flow. - The variation of ihp - php (indicated horsepower minus engine pumping horsepower) with charge-air flow is shown in figure 9. Separate plots are included for each fuel-air ratio. Each plot is keyed according to engine speed and the data obtained over the range of exhaust pressures at each inlet-manifold pressure are included in the points

shown. At constant fuel-air ratio, ihp - php is proportional to charge-air flow independent of engine speed and inlet-manifold pressure. The plot for a fuel-air ratio of 0.085 (fig. 9(b)) has the greatest slope of those presented.

Effect of exhaust pressure on inlet-manifold mixture temperature. - The investigation showed that for constant carburetor-air temperature, engine speed, and fuel-air ratio, the inlet-manifold mixture temperature increased as the engine exhaust pressure was increased. This effect is illustrated in figure 10 where the difference between inlet-manifold mixture temperature and carburetor-air temperature $T_m - T_c$ is plotted against p_e/p_m. The use of the temperature difference $T_m - T_c$ as the ordinate serves to eliminate small variations in carburetor-air temperature experienced during the individual runs. The curves show the effect of p_e/p_m on inlet-manifold mixture temperature to be considerably more pronounced at low engine speeds than high and essentially independent of inlet-manifold pressure.

As previously noted, the brake horsepower curves of figure 5 have been corrected to a constant carburetor-air temperature and, hence, include the effect of the varying inlet-manifold mixture temperature. The curves of ϕ (fig. 4), which were corrected to a constant inlet-manifold mixture temperature, do not include this variation. For comparison, curves of ϕ corrected to constant carburetor-air temperature (variable inlet-manifold temperature) are shown in figure 11 for several engine speeds with corresponding curves corrected to constant mixture temperature from figure 4.

Comparison of the curves shows that operation at constant T_c causes a greater change in power with exhaust pressure than operation at constant T_m; the effect becomes less pronounced as the engine speed increases. The absolute level of ϕ for constant T_c is higher than for constant T_m at low engine speeds where $T_m - T_c$ is small (low impeller tip speed) and the inlet-manifold mixture temperatures corresponding to a 550° R carburetor-air temperature are less than 660° R. The trend is reversed at high speed (3000 rpm) where the inlet-manifold temperature for T_c of 550° R is greater than 660° R.

Effect of exhaust pressure on exhaust-gas temperature. - Exhaust-gas temperatures are plotted against p_e/p_m in figure 12 for various engine operating conditions. The temperatures reach a peak at a value of p_e/p_m between 0.6 and 1.0. Exhaust-gas temperature increases with engine speed and inlet-manifold pressure and increases when the fuel-air ratio decreases from 0.100 to 0.069.

Effect of exhaust pressure on cylinder-head temperature. - The variation of average cylinder-head temperature between exhaust valves with p_e/p_m is presented in figure 13 for representative engine conditions. The curves shown are for constant inlet-manifold pressure and are quite flat over the range of exhaust pressure. Operation at constant weight of charge would, however, result in continuous increase of cylinder-head temperature with p_e/p_m throughout the reported range.

Effect of exhaust pressure on heat rejected to coolant. - A plot of heat rejected to the coolant against p_e/p_m is shown in figure 14 for constant values of engine speed, inlet-manifold pressure, and fuel-air ratio. Heat rejection curves like those of cylinder-head temperature are fairly flat with p_e/p_m. The heat rejection per pound of charge, however, increases with p_e/p_m throughout the range covered.

Comparison of effects of exhaust pressure on 12-cylinder liquid-cooled and 18-cylinder air-cooled engines. - Faired curves of the ratio α (where α is defined as the ratio of brake horsepower at any value of p_e/p_m to the value of brake horsepower at $p_e/p_m = 1.0$ for the same engine speed, fuel-air ratio and altitude), against p_e/p_m for the liquid-cooled engine and the models of the 18-cylinder, air-cooled, radial engine of references 2 and 3 all operating at the same nominal conditions are shown in figure 15. The curves are presented for the purpose of comparing the effect of exhaust pressure on the brake horsepower of the three different engines.

This figure shows that the two engines with the higher valve overlaps are more sensitive to exhaust pressure than is the engine with the lowest valve overlap. The liquid-cooled engine with 74° valve overlap and the air-cooled engine with 62° overlap produce curves of the same general shape for the ranges of exhaust to inlet-manifold pressure ratio studied The similarity in curve trends between these two engines was also observed for power, volumetric efficiency, and exhaust-gas temperature.

SUMMARY OF RESULTS

A dynamometer-stand investigation conducted on a 12-cylinder liquid-cooled engine at various engine speeds from 1600 to 3000 rpm, inlet-manifold pressures from 30 to 50 inches of mercury absolute, and fuel-air ratios from 0.063 to 0.100 at exhaust pressures from about 7 to approximately 62 inches of mercury absolute indicated that:

1. At constant engine speed and fuel-air ratio, the ratio of indicated mean effective pressure to inlet-manifold pressure, when

plotted against the ratio of exhaust to inlet-manifold pressure, was nearly independent of inlet-manifold pressure and decreased as exhaust pressure increased.

2. At constant engine speed, fuel-air ratio, and carburetor-air temperature, the inlet-manifold mixture temperature increased with increasing exhaust pressure. The trend was more marked at low engine speeds than high.

3. The volumetric efficiency and the difference between inlet-manifold and carburetor-air temperature were also essentially independent of inlet-manifold pressure for constant values of the ratio of exhaust to inlet-manifold pressure.

4. Exhaust-gas temperature reached a maximum at values of the ratio of exhaust to inlet-manifold pressure between 0.6 and 1.0.

5. Curves of heat rejected to the coolant and the average cylinder-head temperature between exhaust valves were fairly constant over the range of exhaust to inlet-manifold pressure ratios. Operation at constant weight of charge, however, would result in continuous increase of heat rejection and cylinder-head temperature with increase in the ratio of exhaust to inlet-manifold pressure throughout the range.

Flight Propulsion Research Laboratory,
National Advisory Committee for Aeronautics,
Cleveland, Ohio, May 1, 1947.

REFERENCES

1. Pinkel, Benjamin: Effect of Exhaust Back Pressure on Engine Power. NACA CB No. 3F17, 1943.

2. Boman, David S., Nagey, Tibor F., and Doyle, Ronald B.: Effect of Exhaust Pressure on the Performance of an 18-Cylinder Air-Cooled Radial Engine with a Valve Overlap of 40°. NACA TN No. 1220, 1947.

3. Humble, Leroy V., Nagey, Tibor F., and Boman, David S.: Effect of Exhaust Pressure on the Performance of an 18-Cylinder Air-Cooled Radial Engine with a Valve Overlap of 62°. NACA TN No. 1232, 1947.

4. Moore, Charles S., Biermann, Arnold E., and Voss, Fred: The NACA Balanced-Diaphragm Dynamometer-Torque Indicator. NACA RB No. 4C28, 1944.

5. Cragoe, C. S.: Properties of Ethylene Glycol and Its Aqueous Solutions. Cooperative Fuel Res. Committee, CRC, July 1943.

TABLE I - OPERATING CONDITIONS

Nominal engine speed (rpm)	Nominal fuel-air ratio	Nominal inlet-manifold pressure (in. Hg absolute)	Remarks
1600 2000 2400 2600 3000	0.085	30	
1600 2000 2400 2600 3000	0.069	30	
1600 2000 2400 2600	0.063	30	
1600 2000 2400 2600 3000	0.100	40	
1600 2000 2400 2600 3000	0.085	40	
1600 2000 2400 2600 3000	0.069	40	Surge at p_e = 51 in. Hg absolute Surge at p_e = 60 in. Hg absolute Incipient detonation at p_e = 45 in. Hg absolute No detonation up to p_e = 49 in. Hg absolute
1600 2000 2400 2600	0.063	40	 Surge at p_e = 47 in. Hg absolute Incipient detonation at p_e = 49 in. Hg absolute Incipient detonation at p_e = 45 in. Hg absolute
2400 2600 3000	0.100	50	
2400 2600 3000	0.085	50	

National Advisory Committee for Aeronautics

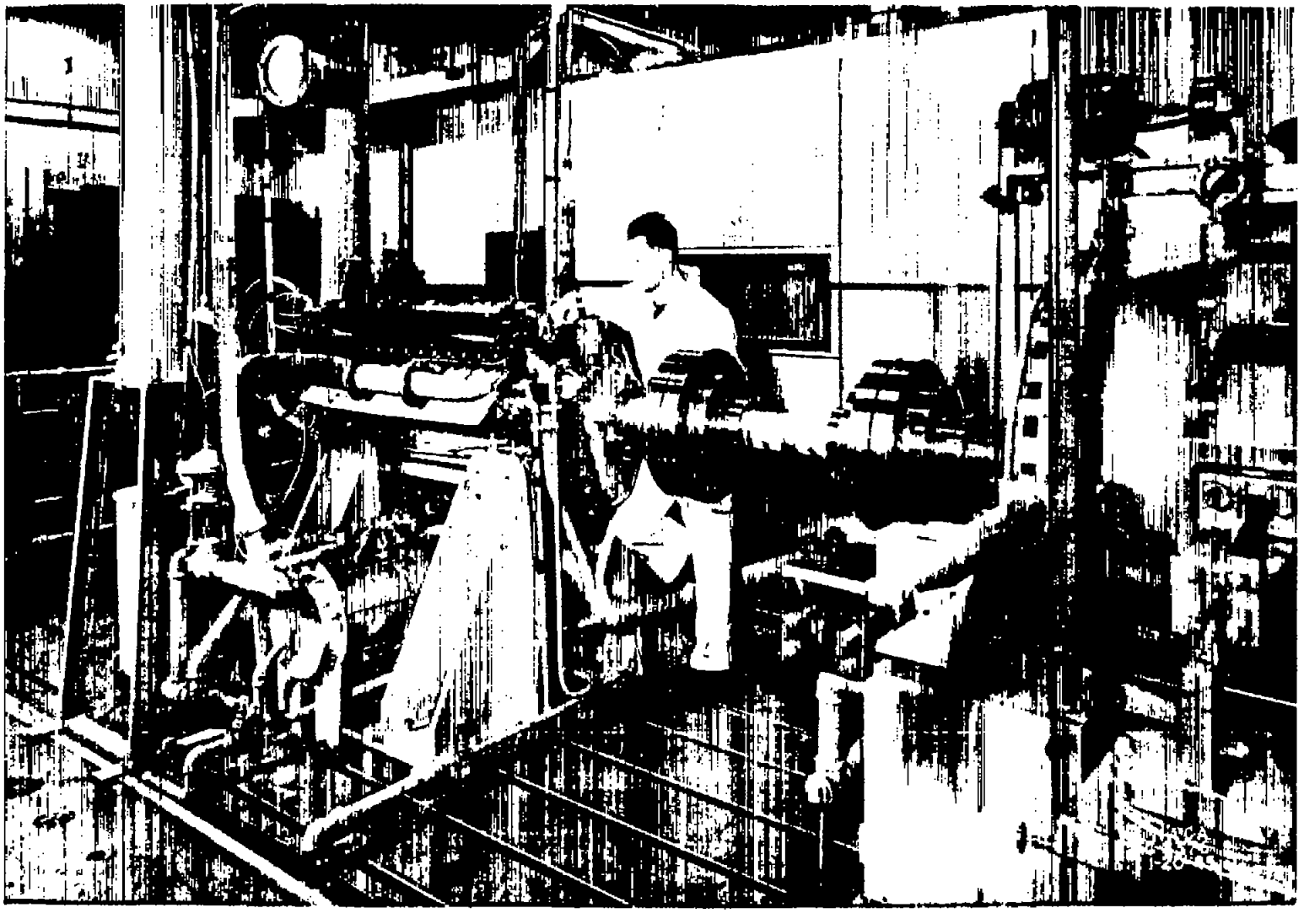

Figure 1. - General view of engine installation.

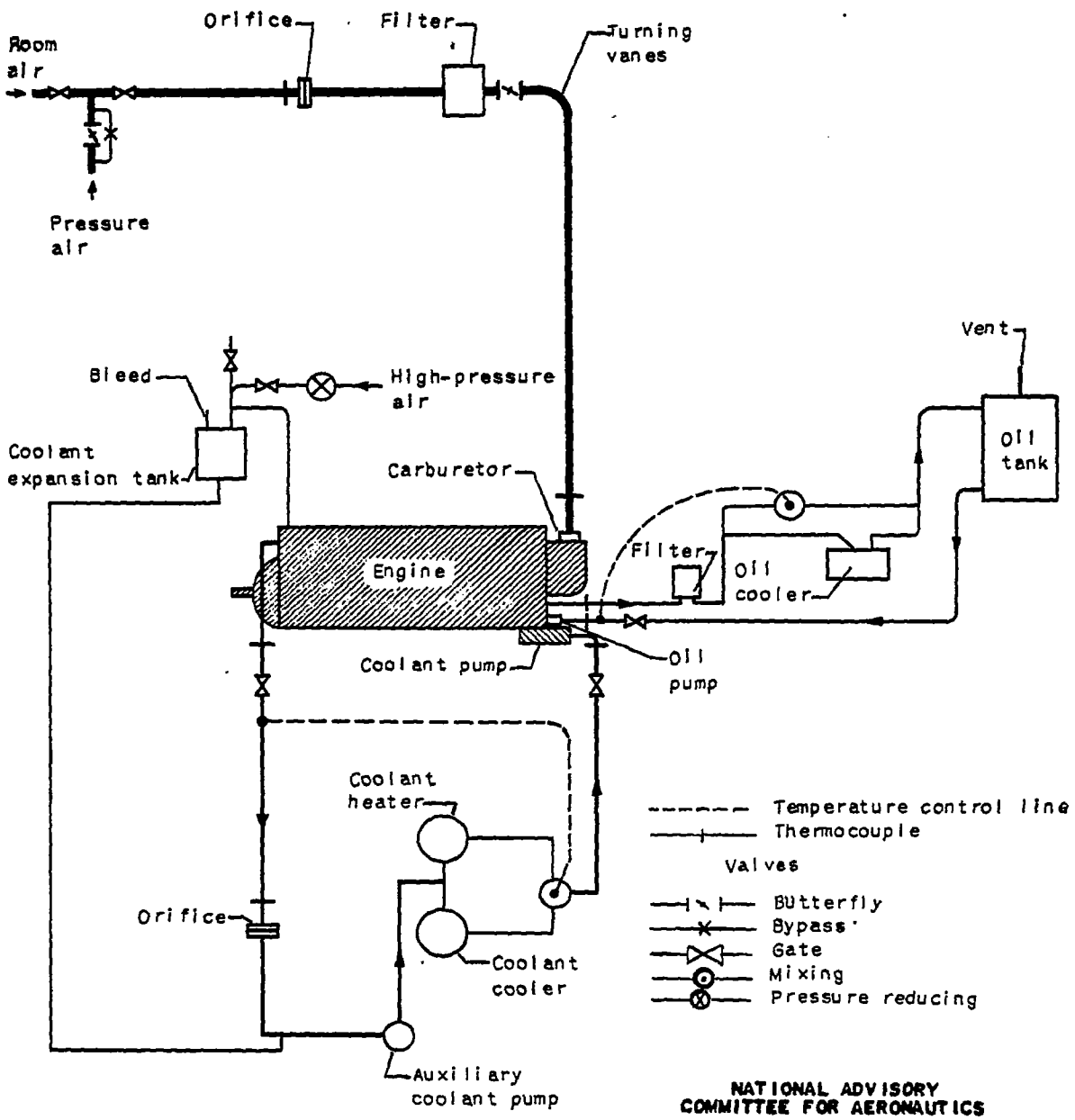

Figure 2. - Schematic diagram showing combustion-air, engine-oil, and coolant systems.

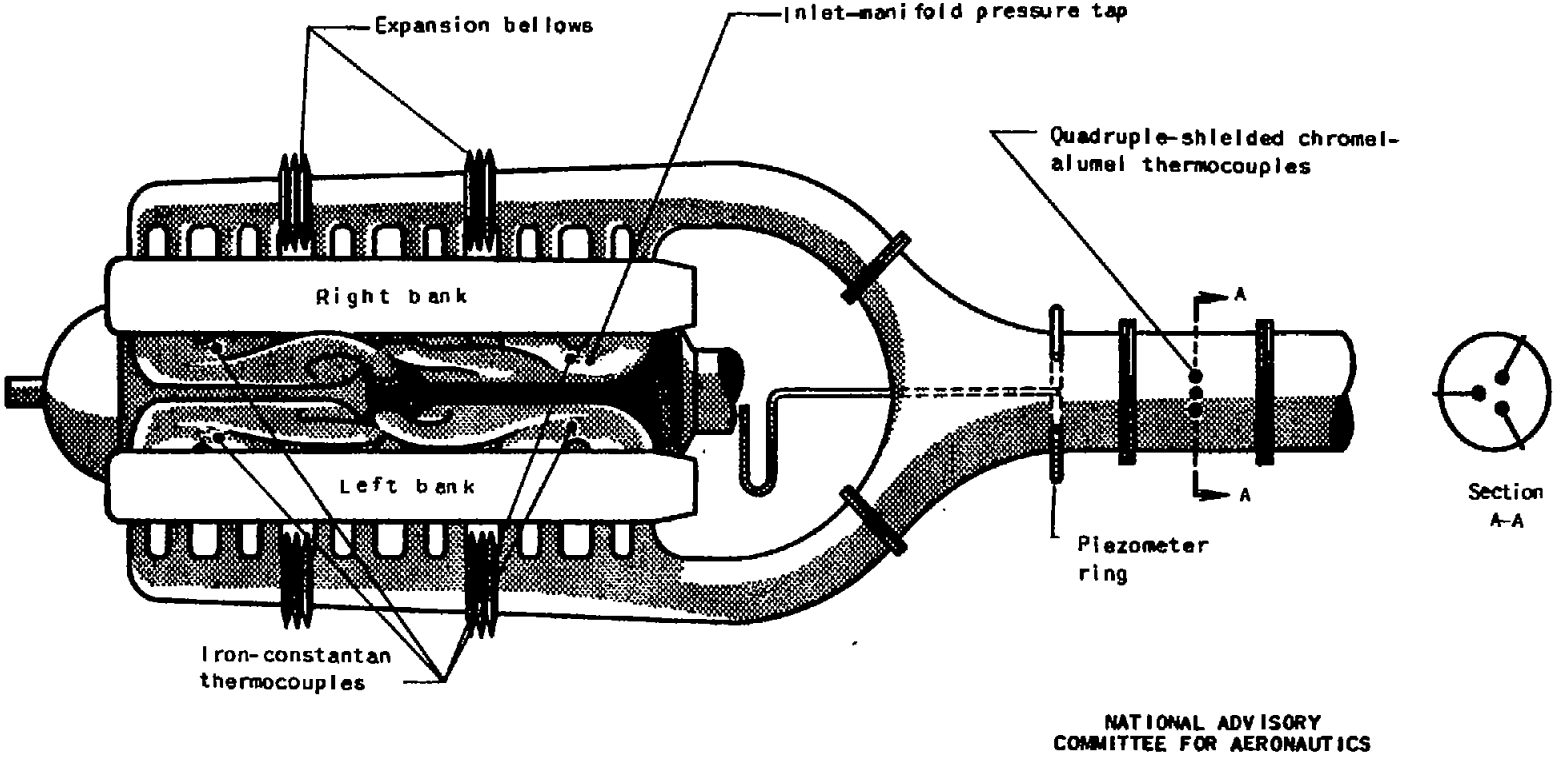

Figure 3. - Schematic diagram of inlet-manifold and exhaust systems showing locations at which pressure and temperature measurements were taken.

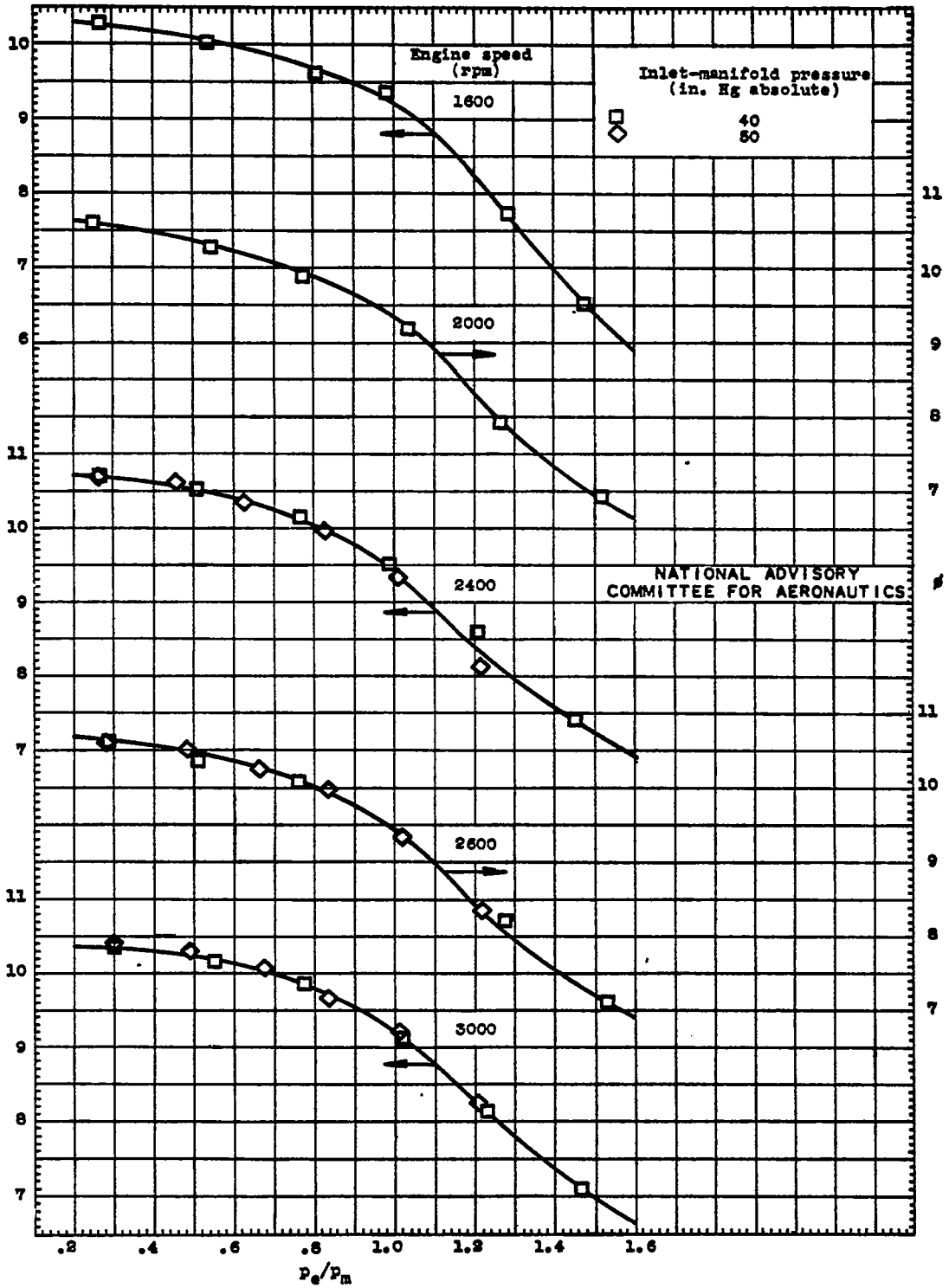

(a) Fuel-air ratio, 0.100.

Figure 4. - Variation of ϕ with p_e/p_m for constant engine speeds. Values of ϕ corrected to constant inlet-manifold mixture temperature T_m of 660° R.

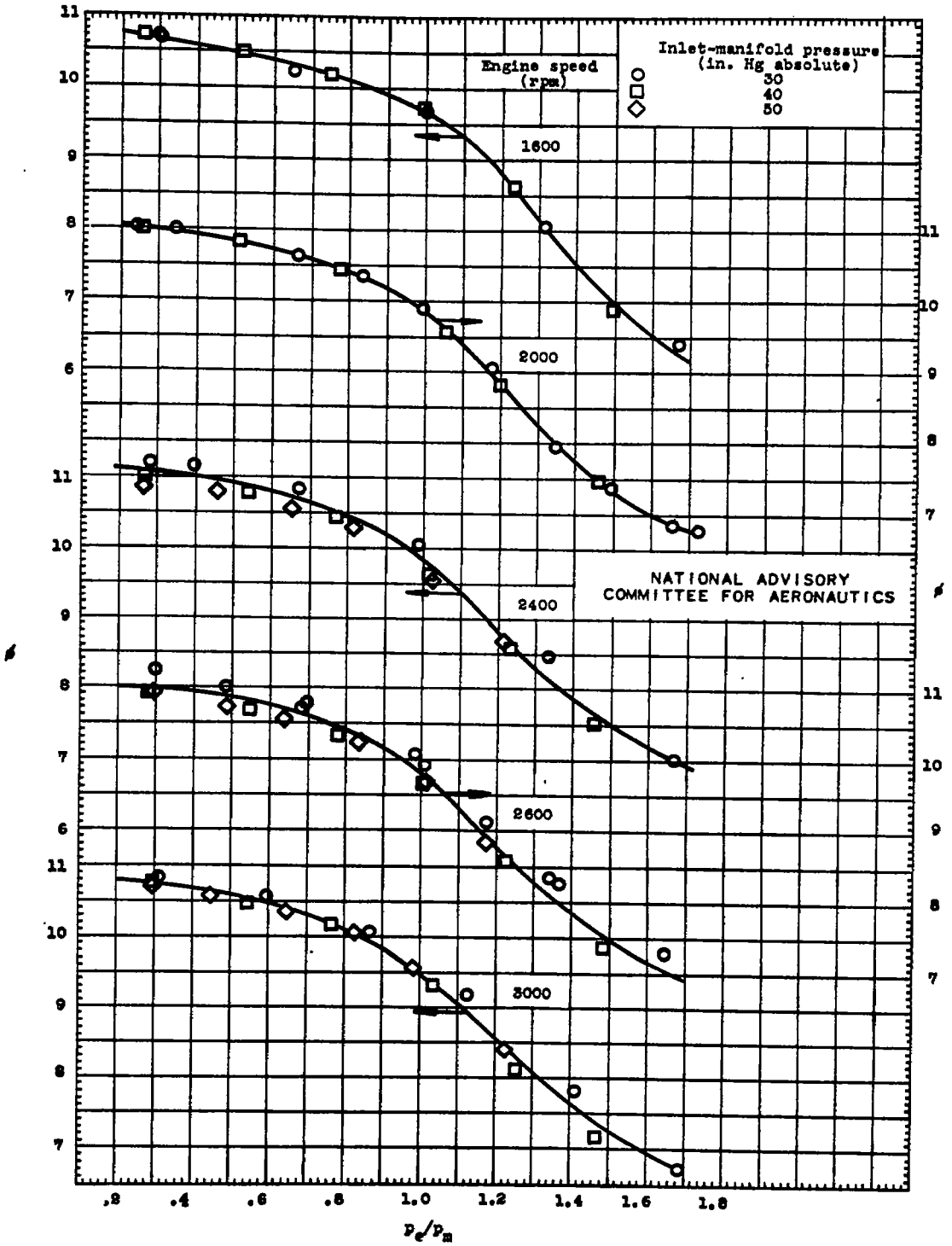

(b) Fuel-air ratio, 0.065.

Figure 4. - Continued. Variation of ϕ with p_e/p_m for constant engine speeds. Values of ϕ corrected to constant inlet-manifold mixture temperature T_m of 660° R.

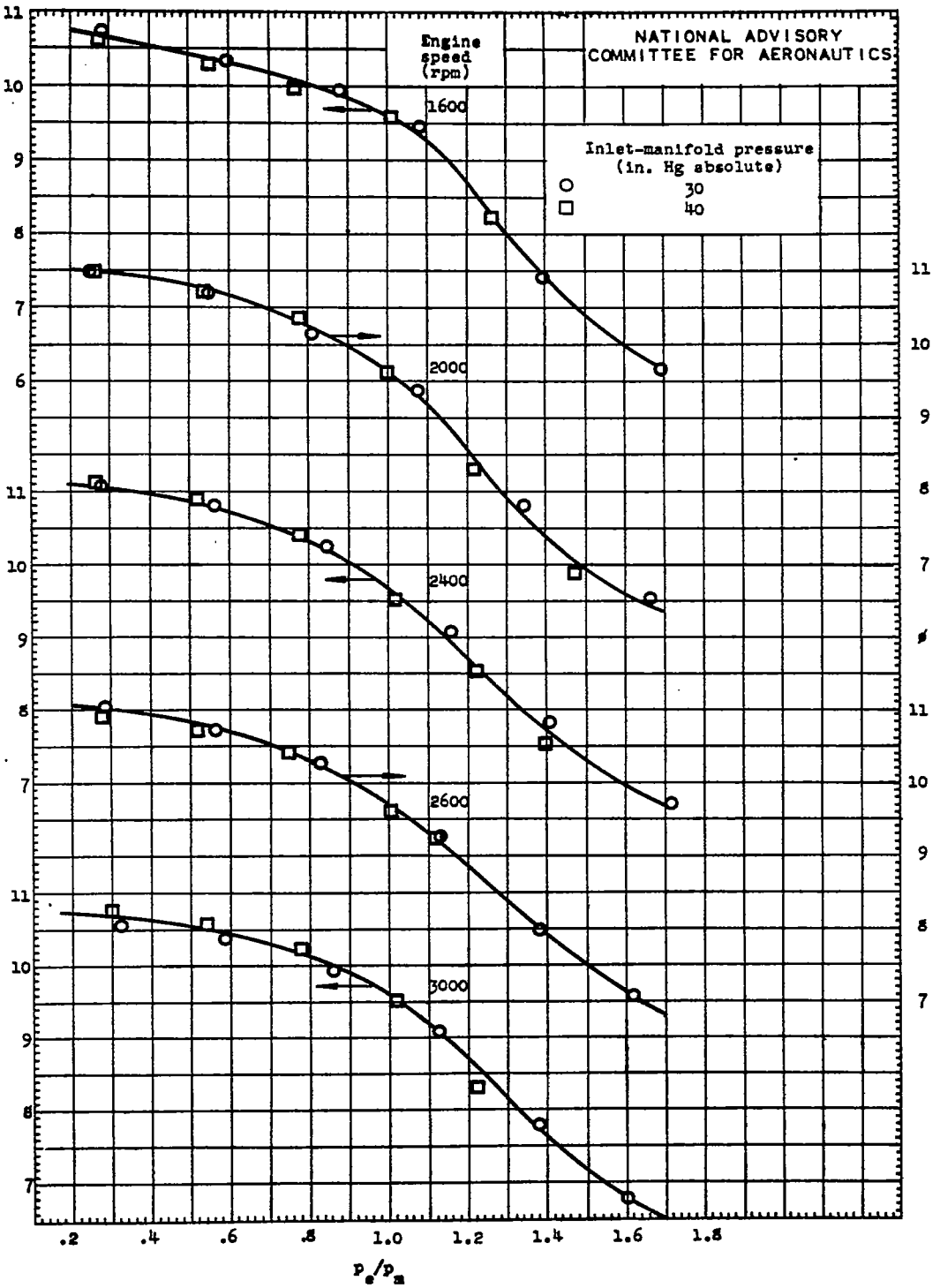

(c) Fuel-air ratio, 0.069.

Figure 4. - Continued. Variation of ϕ with p_e/p_m for constant engine speeds. Values of ϕ corrected to constant inlet-manifold mixture temperature T_m of 660° R.

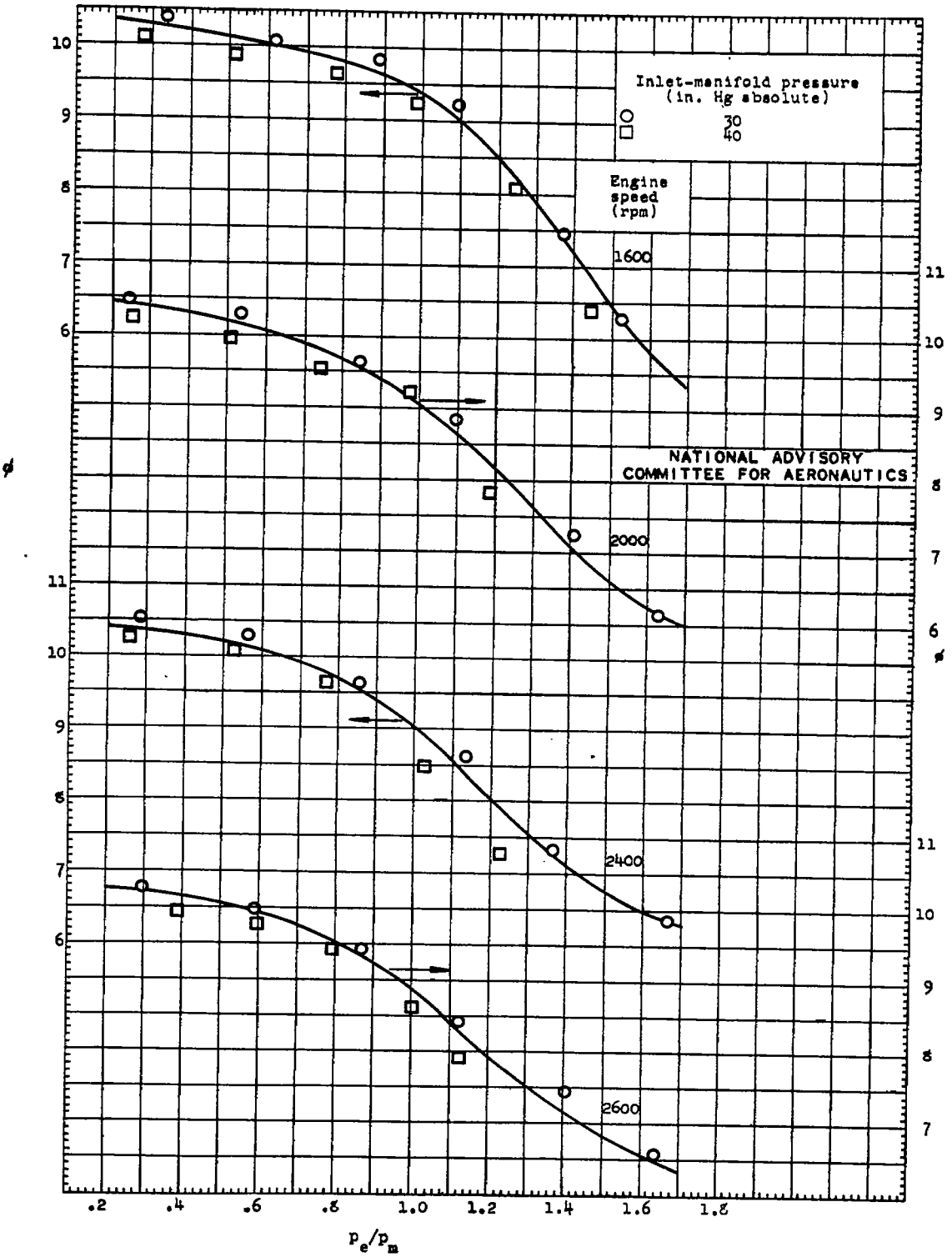

(d) Fuel-air ratio, 0.063.

Figure 4. - Concluded. Variation of ϕ with p_e/p_m for constant engine speeds. Values of ϕ corrected to constant inlet-manifold mixture temperature T_m of 660° R.

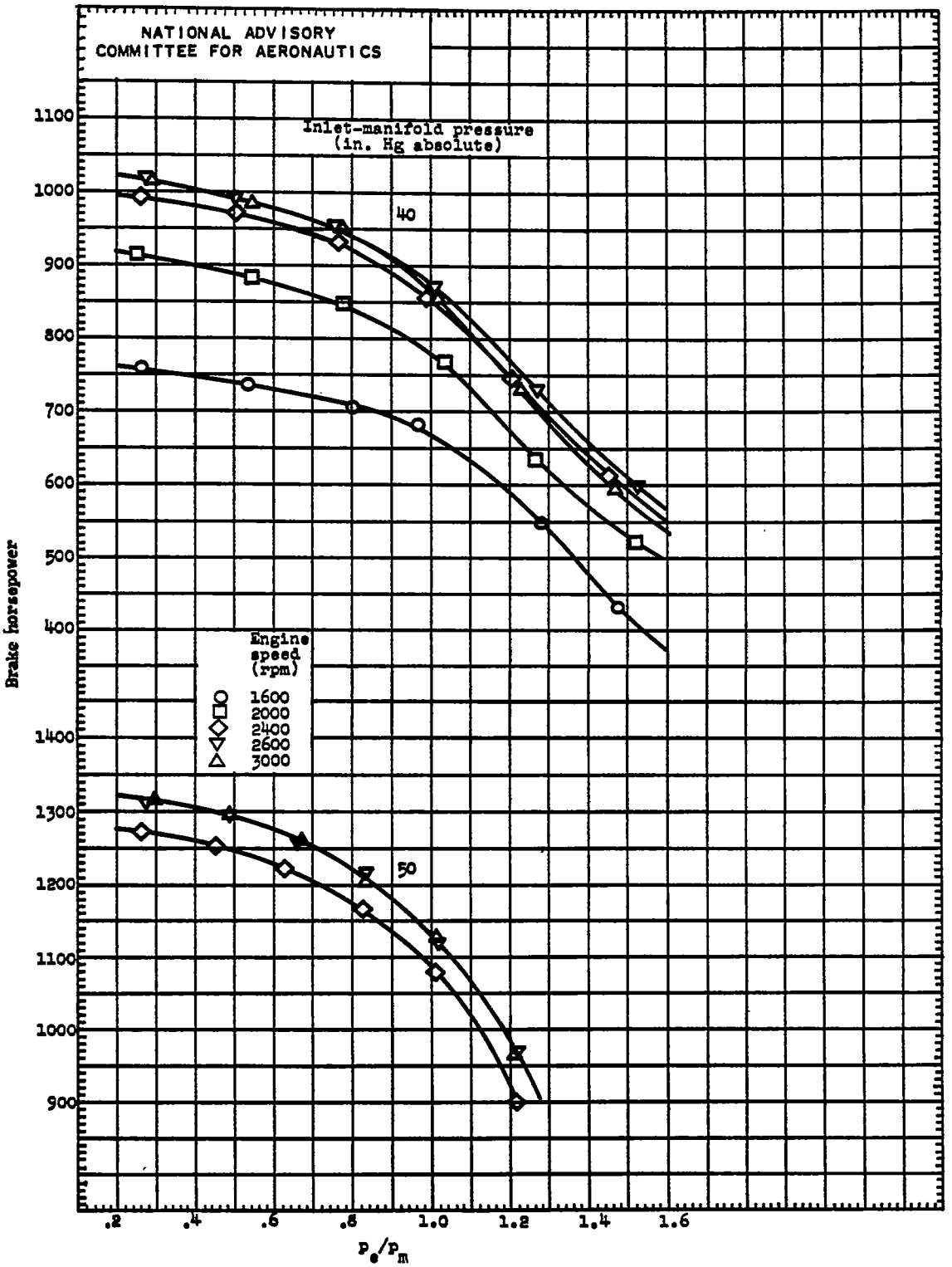

(a) Fuel-air ratio, 0.100.

Figure 5. - Variation of brake horsepower with p_e/p_m for constant engine speeds and inlet-manifold pressures. Brake horsepower corrected to constant carburetor-air temperature T_c of 550° R.

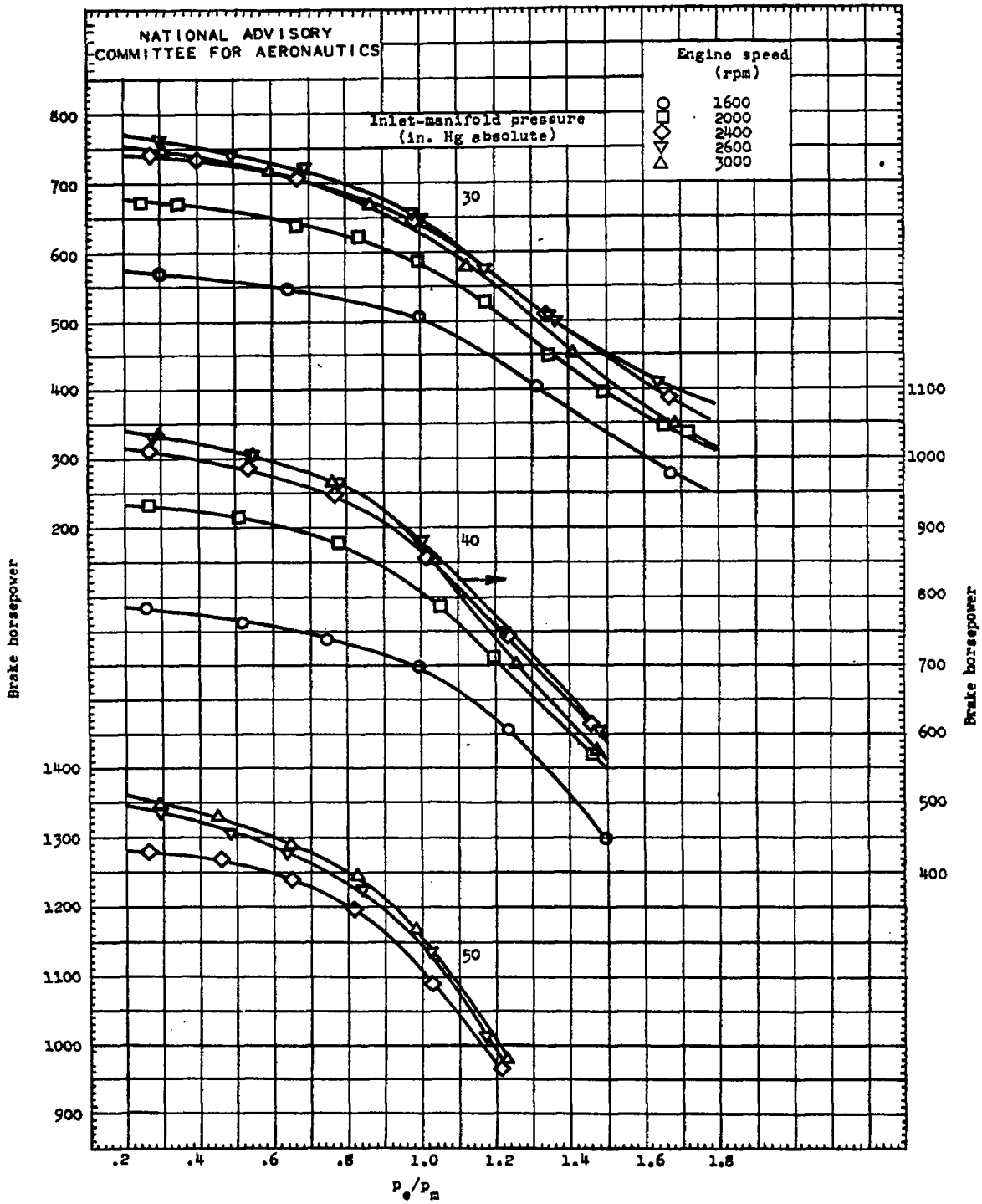

(b) Fuel-air ratio, 0.085.

Figure 5. - Continued. Variation of brake horsepower with p_e/p_m for constant engine speeds and inlet-manifold pressures. Brake horsepower corrected to constant carburetor-air temperature T_c of 550° R.

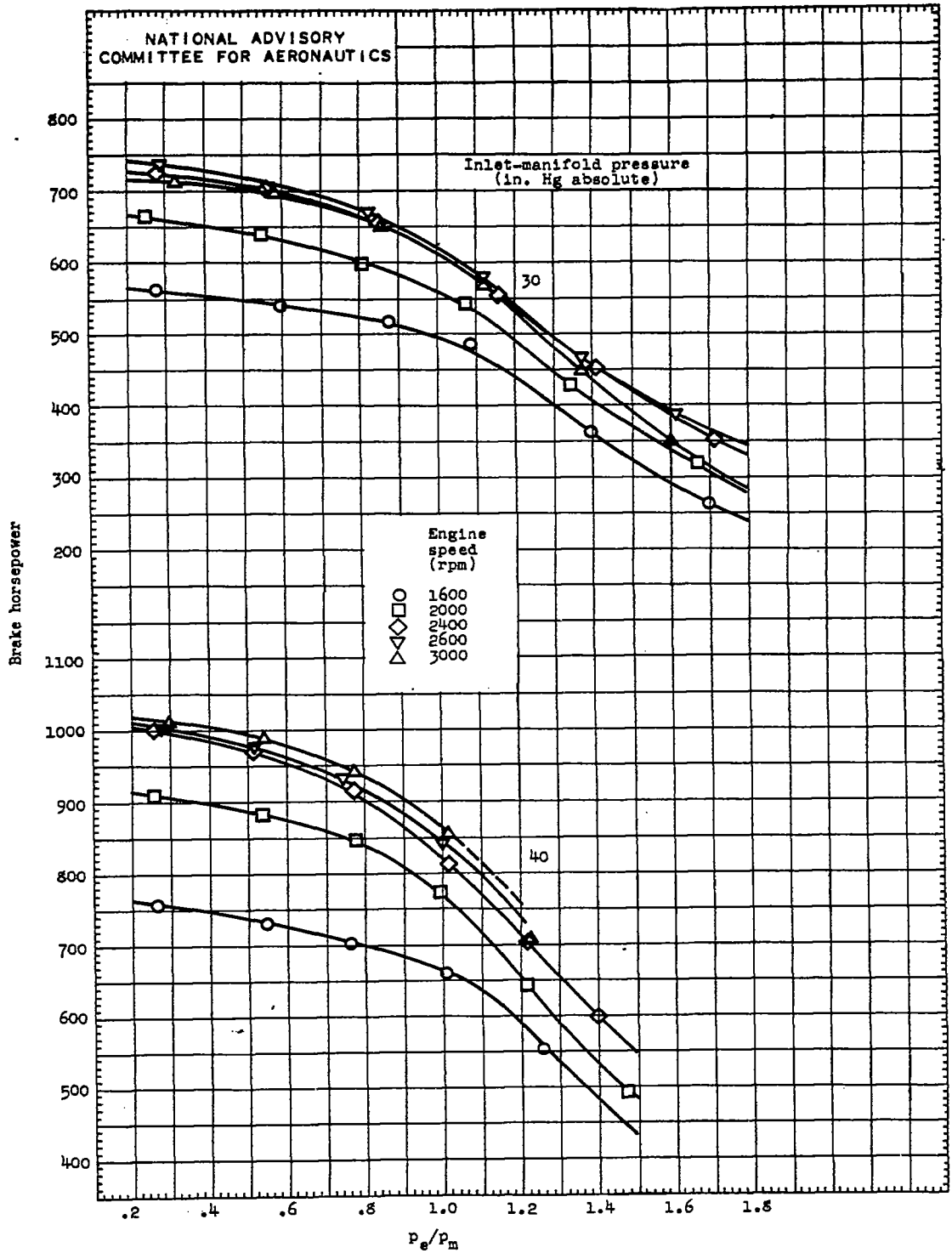

(c) Fuel-air ratio, 0.069.

Figure 5. - Continued. Variation of brake horsepower with p_e/p_m for constant engine speeds and inlet-manifold pressures. Brake horsepower corrected to constant carburetor-air temperature T_c of 550° R.

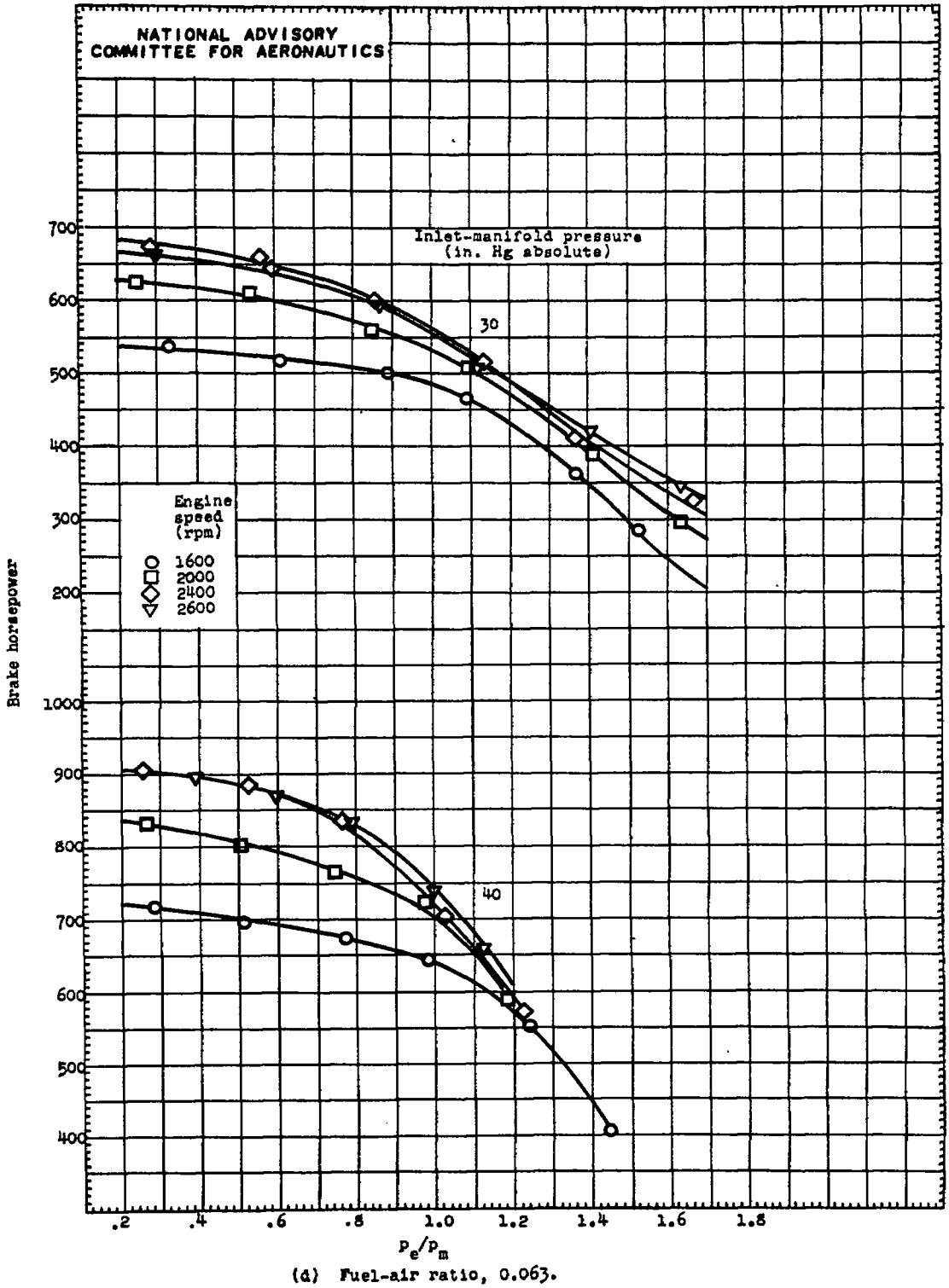

(d) Fuel-air ratio, 0.063.

Figure 5. - Concluded. Variation of brake horsepower with p_e/p_m for constant engine speeds and inlet-manifold pressures. Brake horsepower corrected to constant carburetor-air temperature T_c of 550° R.

754

754

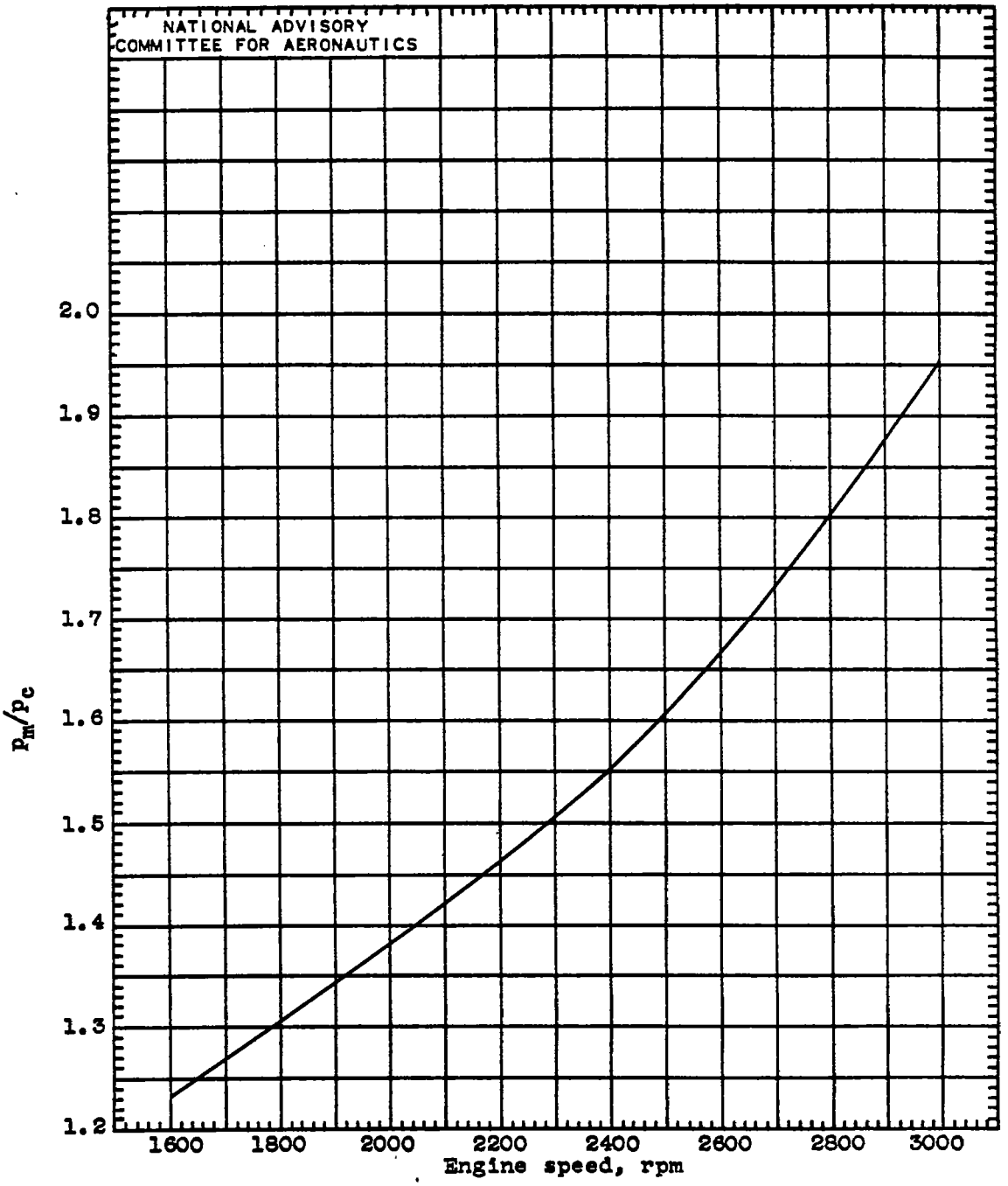

Figure 6. - Variation of p_m/p_c with engine speed. Carburetor-air temperature, 550° ± 15° R.

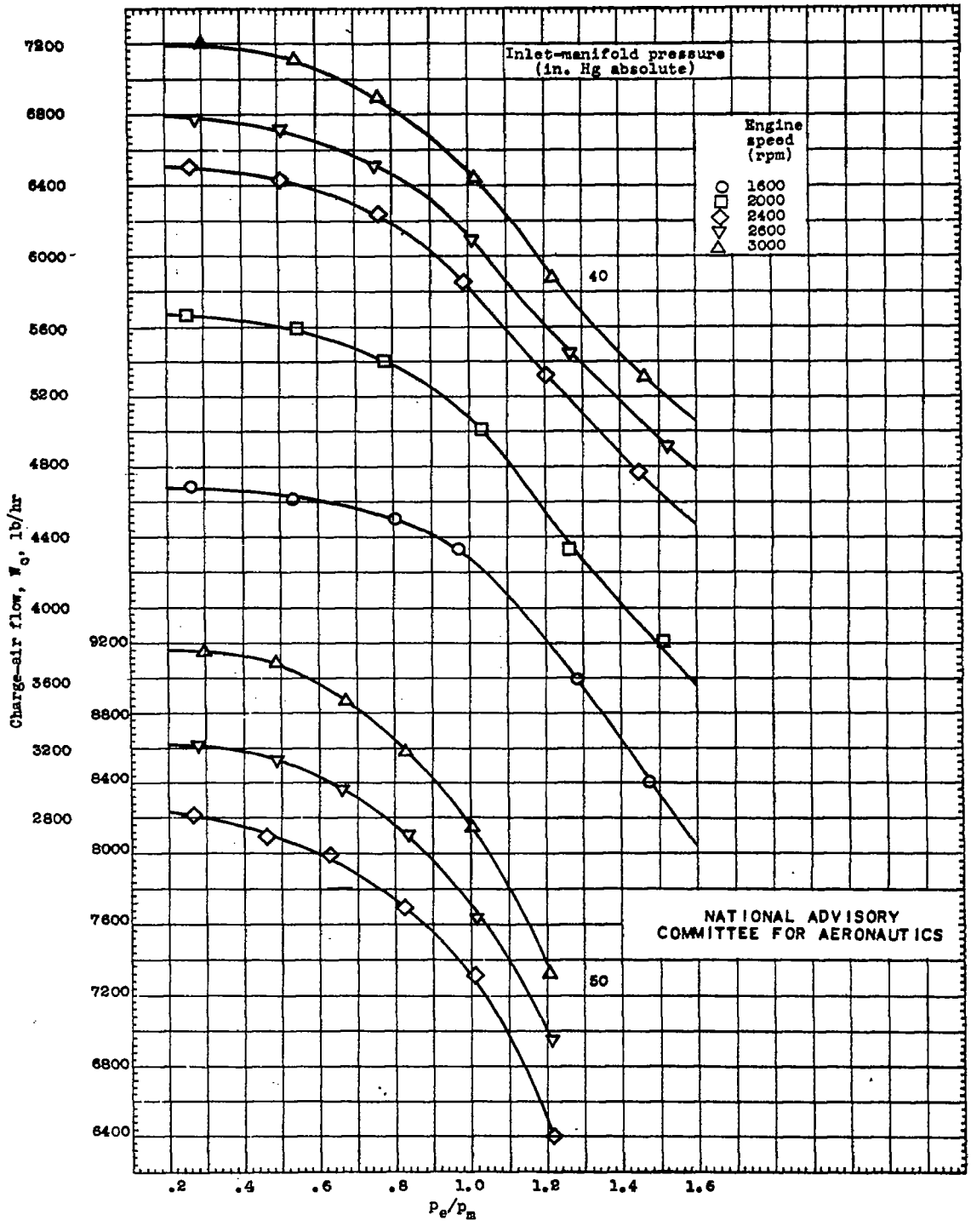

(a) Fuel-air ratio, 0.100.

Figure 7. - Variation of charge-air flow W_c with p_e/p_m for constant engine speeds and inlet-manifold pressures. Charge-air flow corrected to constant carburetor-air temperature T_c of 550° R.

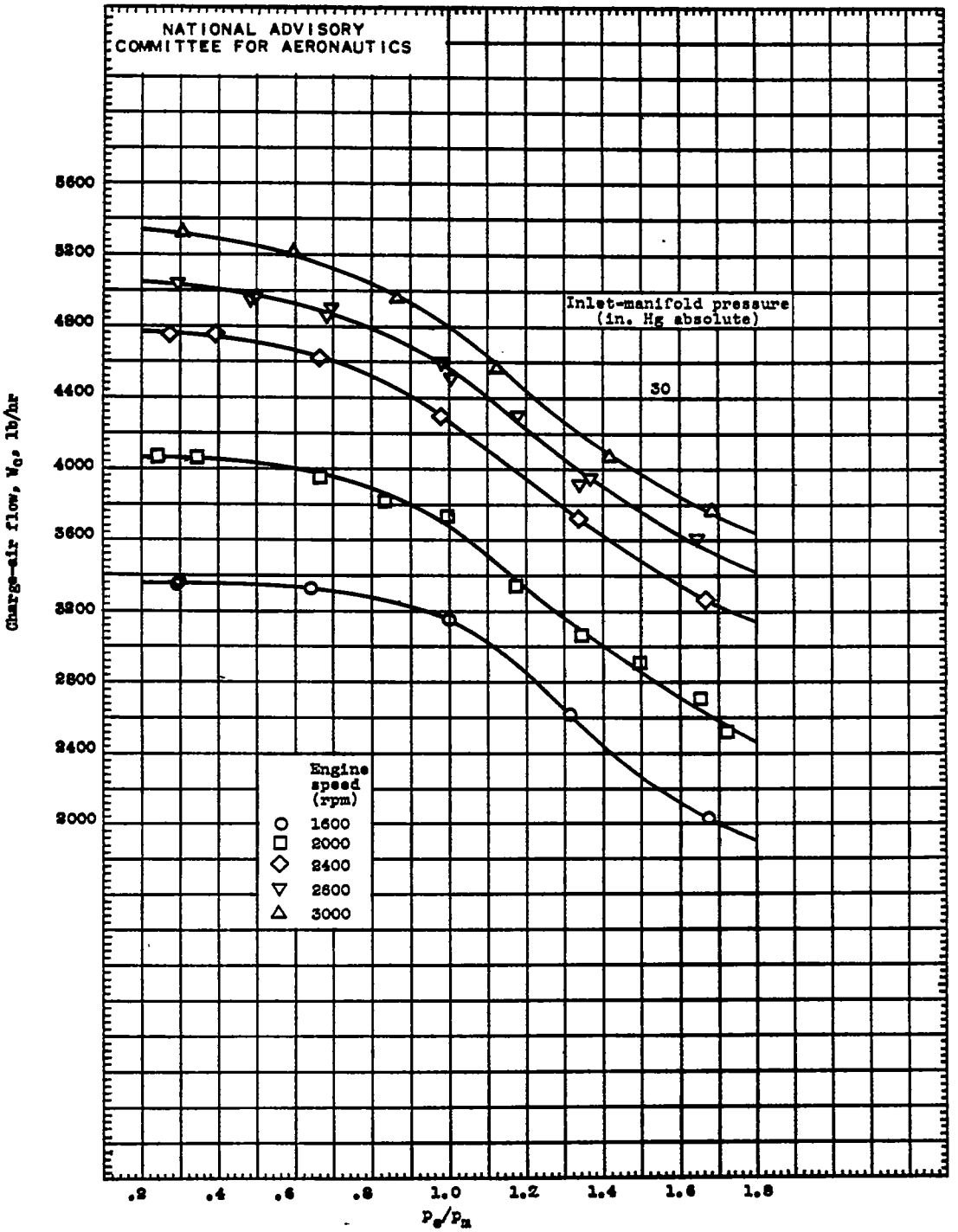

(b) Fuel-air ratio, 0.085

Figure 7. - Continued. Variation of charge-air flow W_c with p_e/p_m for constant engine speeds and inlet-manifold pressures. Charge-air flow corrected to constant carburetor-air temperature T_c of 550° R.

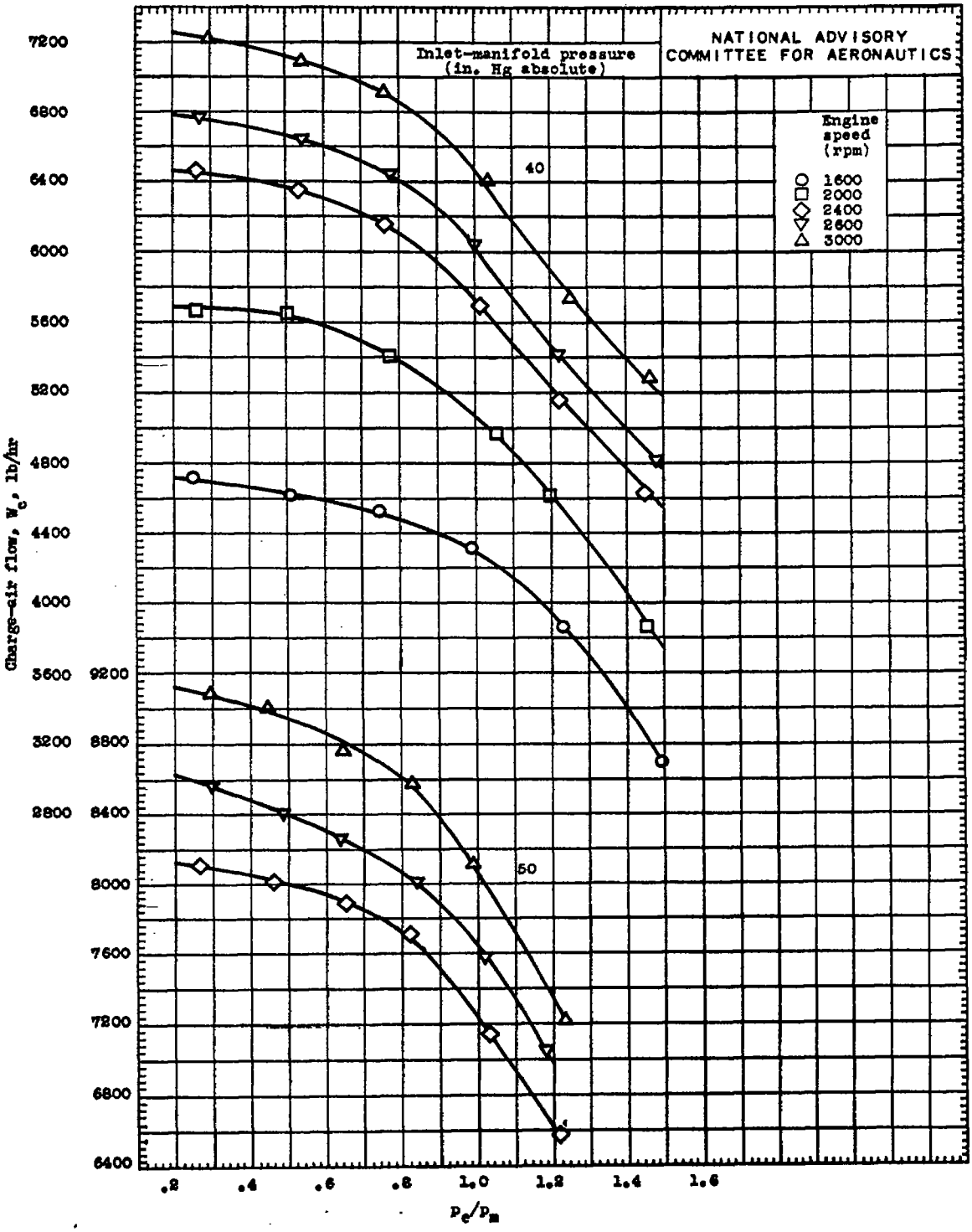

(b) Concluded. Fuel-air ratio, 0.085.

Figure 7. - Continued. Variation of charge-air flow W_c with p_c/p_m for constant engine speeds and inlet-manifold pressures. Charge-air flow corrected to constant carburetor-air temperature T_c of 560° R.

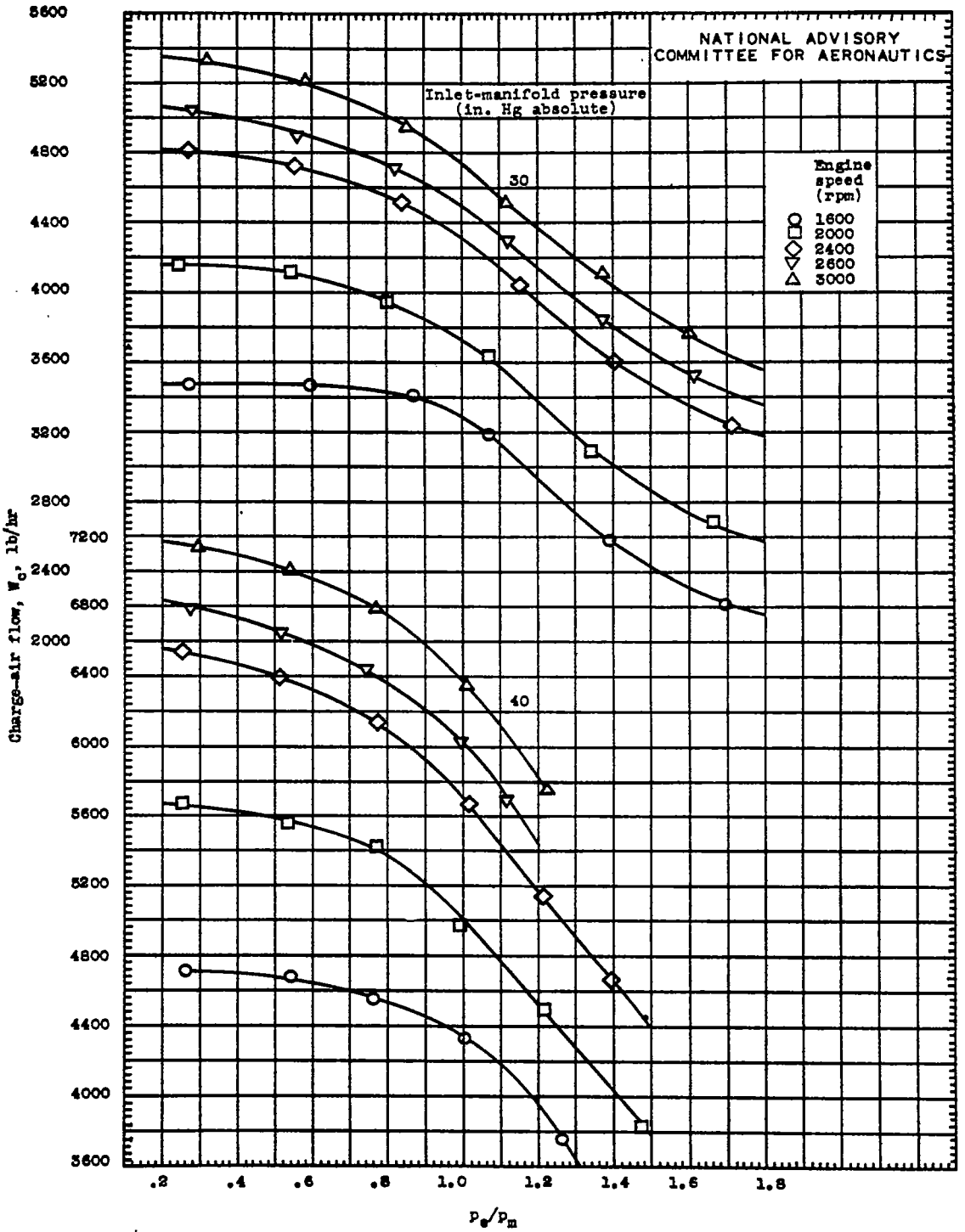

(c) Fuel-air ratio, 0.069.

Figure 7. - Continued. Variation of charge-air flow W_c with p_e/p_m for constant engine speeds and inlet-manifold pressures. Charge-air flow corrected to constant carburetor-air temperature T_c of 550° R.

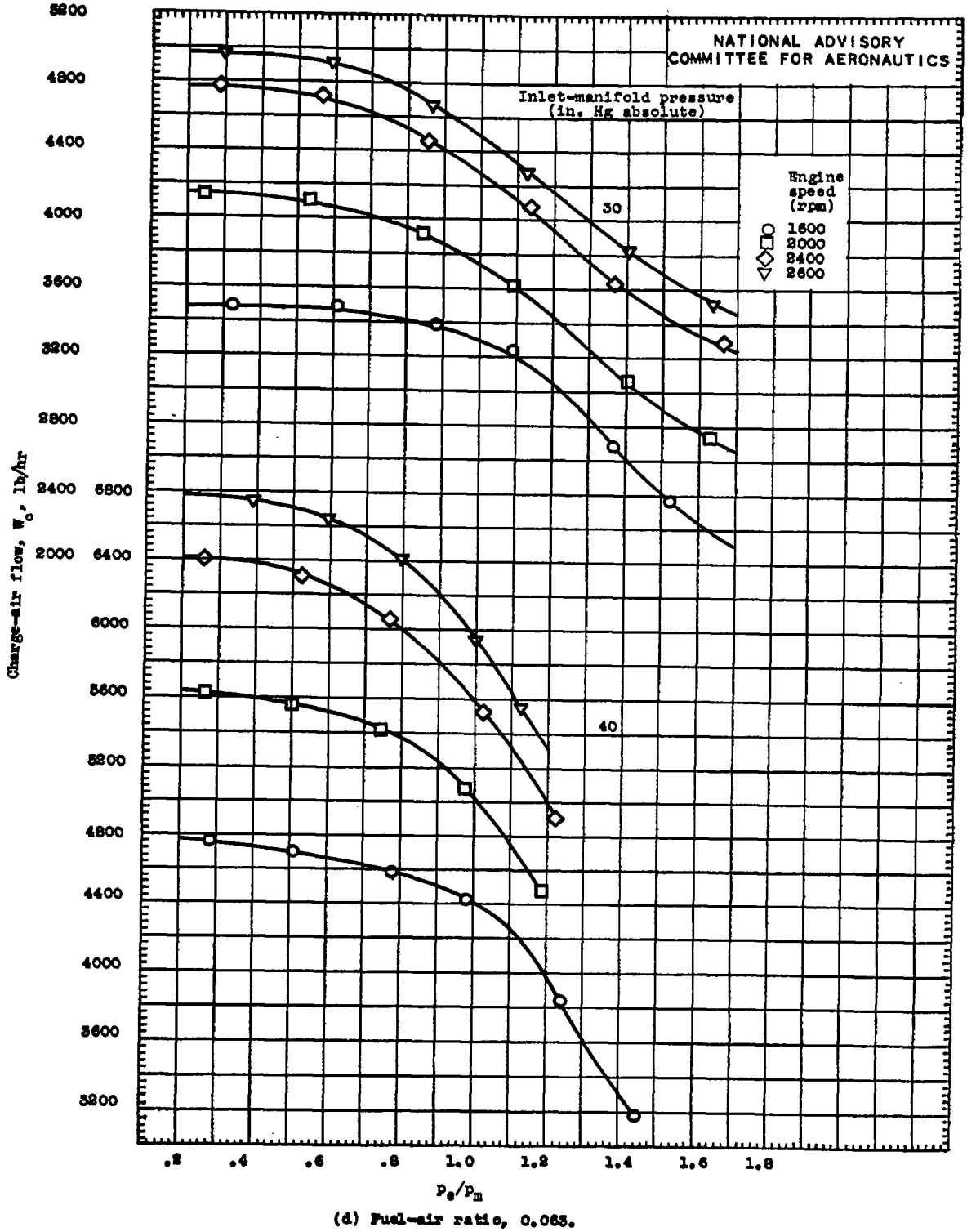

(d) Fuel-air ratio, 0.063.

Figure 7. - Concluded. Variation of charge-air flow W_c with p_e/p_m for constant engine speeds and inlet-manifold pressures. Charge-air flow corrected to constant carburetor-air temperature T_c of 550° R.

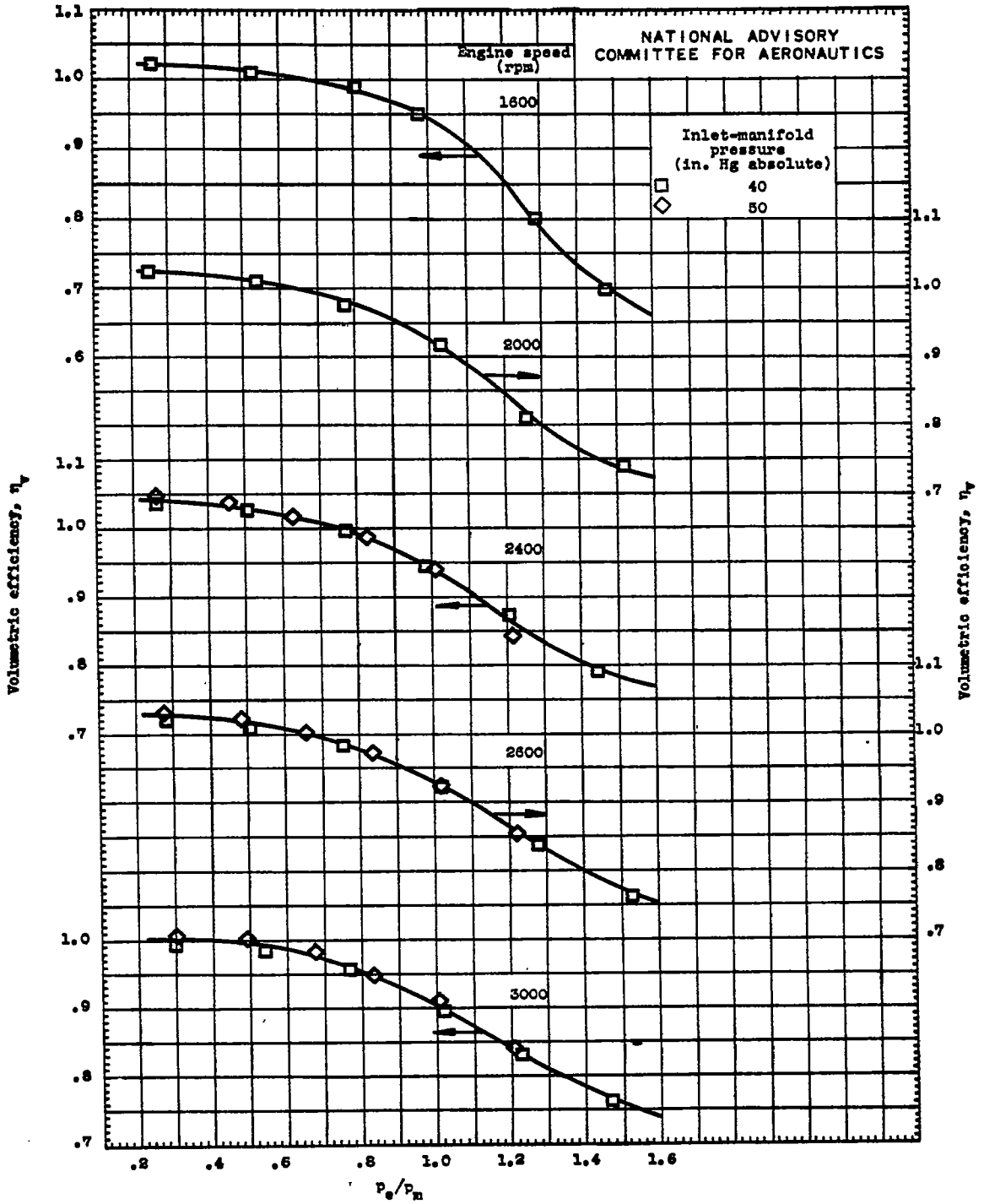

(a) Fuel-air ratio, 0.100.

Figure 8. - Variation of volumetric efficiency η_v with p_e/p_m for constant engine speeds.

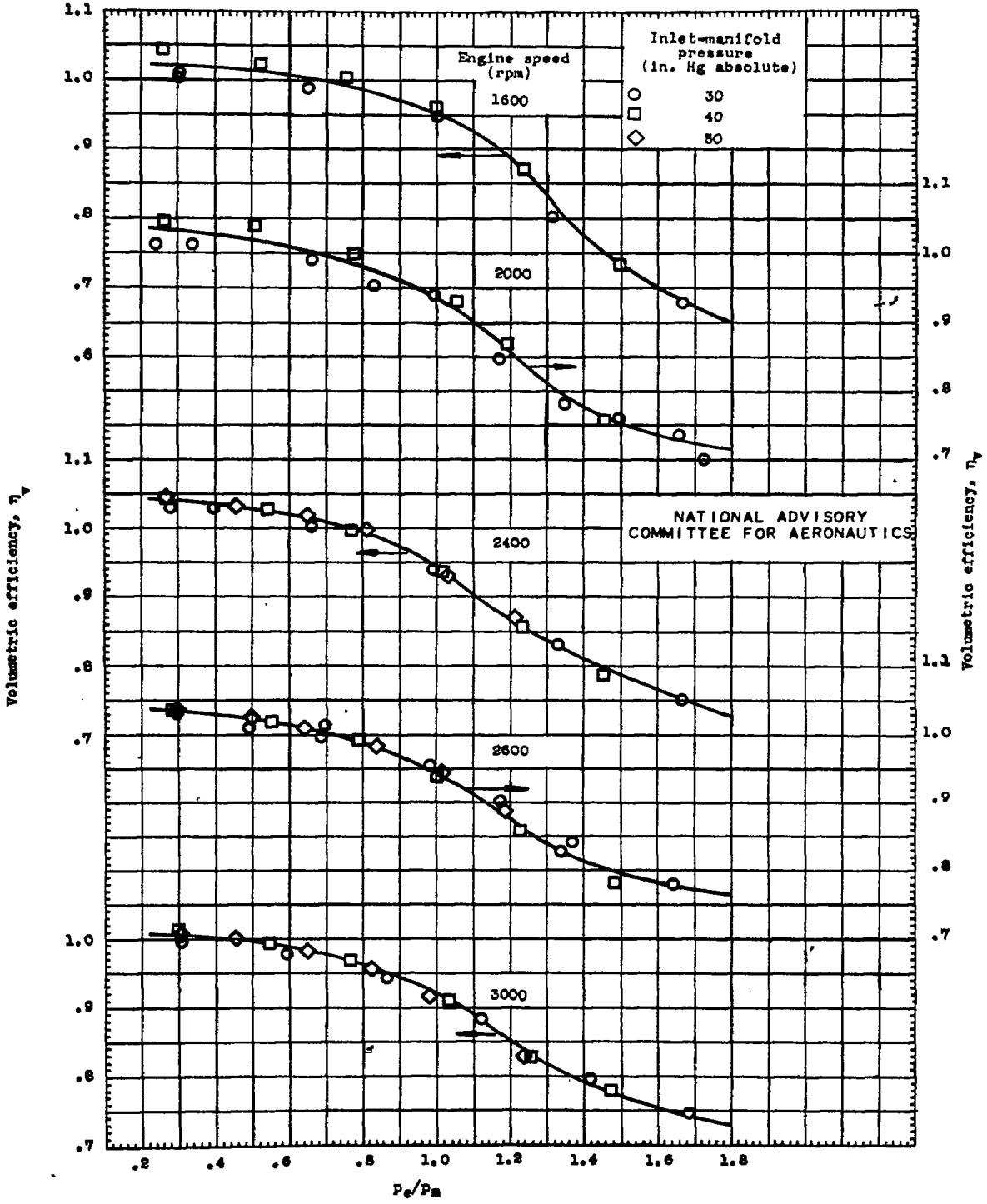

(b) Fuel-air ratio, 0.085.

Figure 8. - Continued. Variation of volumetric efficiency η_v with p_e/p_m for constant engine speeds.

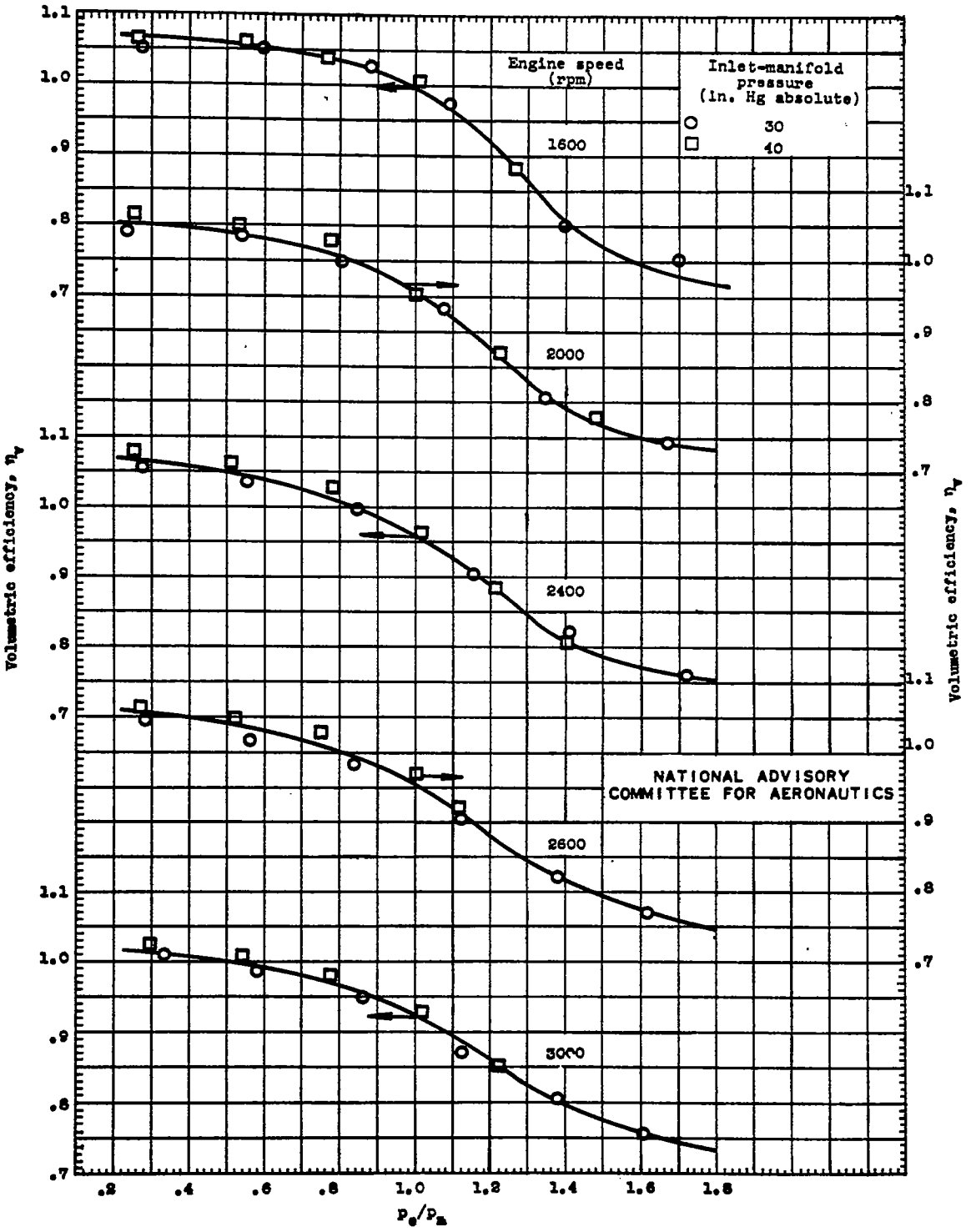

(c) Fuel-air ratio, 0.069.

Figure 8. - Continued. Variation of volumetric efficiency η_v with p_e/p_m for constant engine speeds.

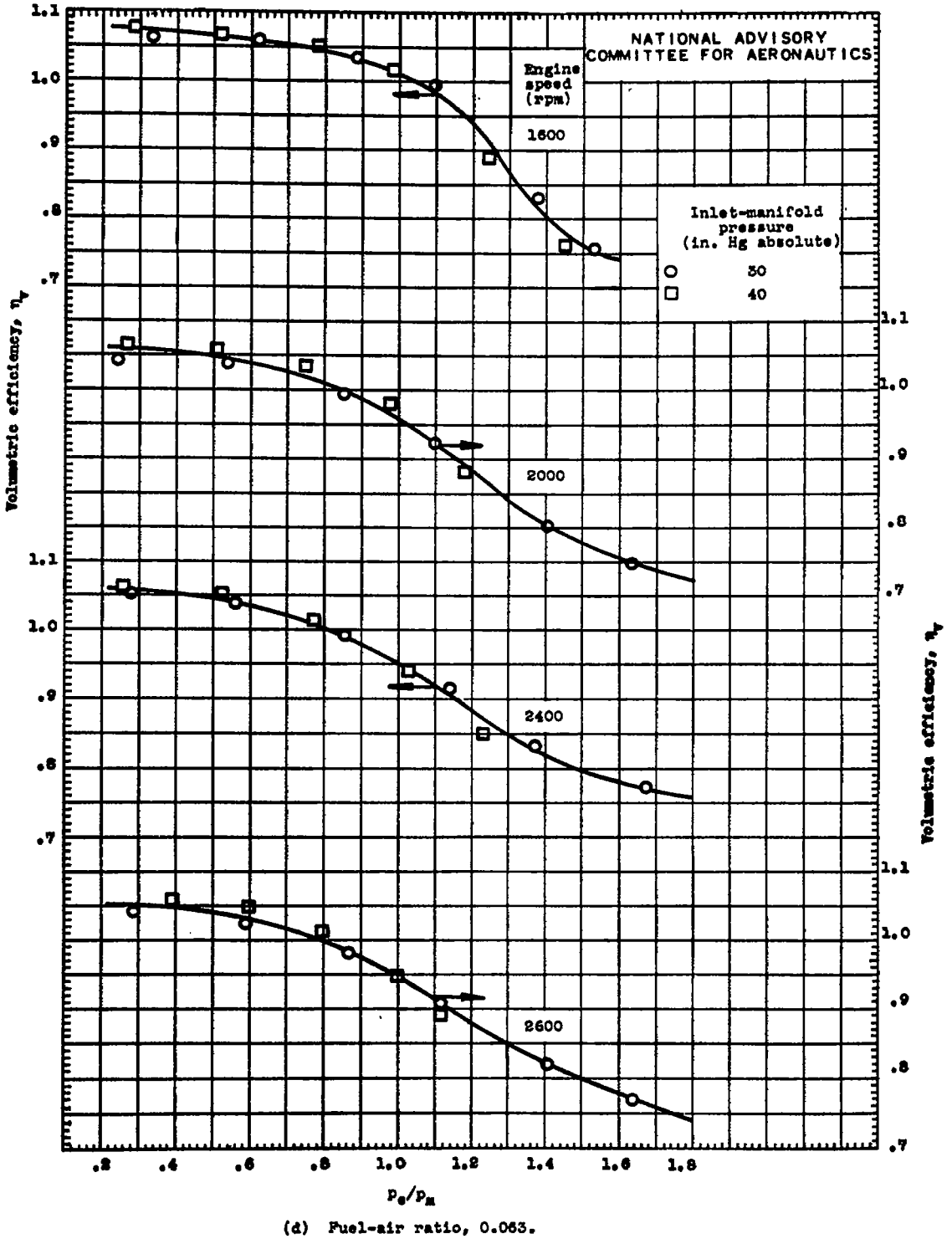

(d) Fuel-air ratio, 0.063.

Figure 8. - Concluded. Variation of volumetric efficiency η_v with p_e/p_m for constant engine speeds.

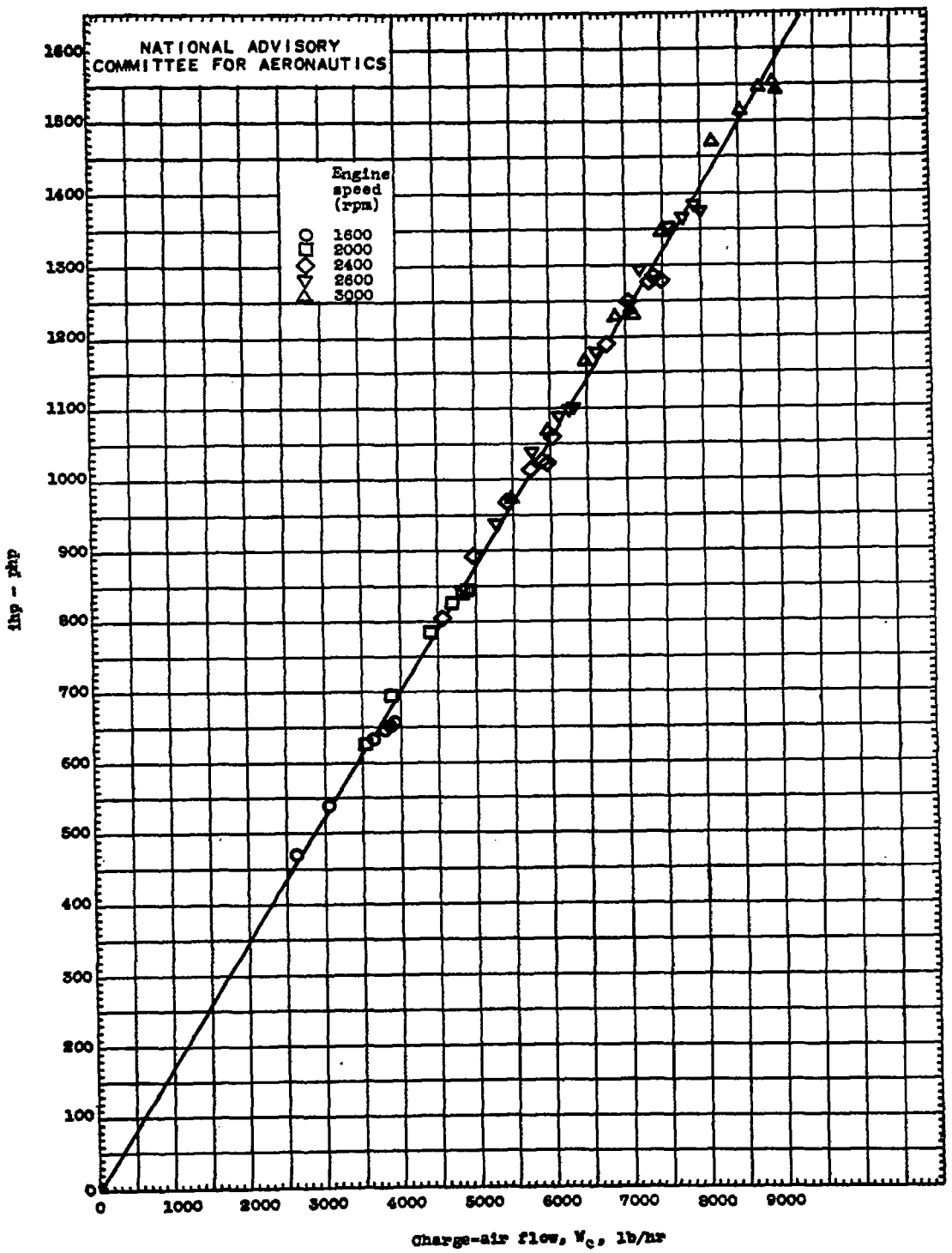

(a) Fuel-air ratio, 0.100.

Figure 9. - Variation of ihp - php with charge-air flow for various engine speeds and values of p_e/p_m. Values of ihp - php and charge-air flow W_c corrected to constant inlet-manifold mixture temperature T_m of 660° R.

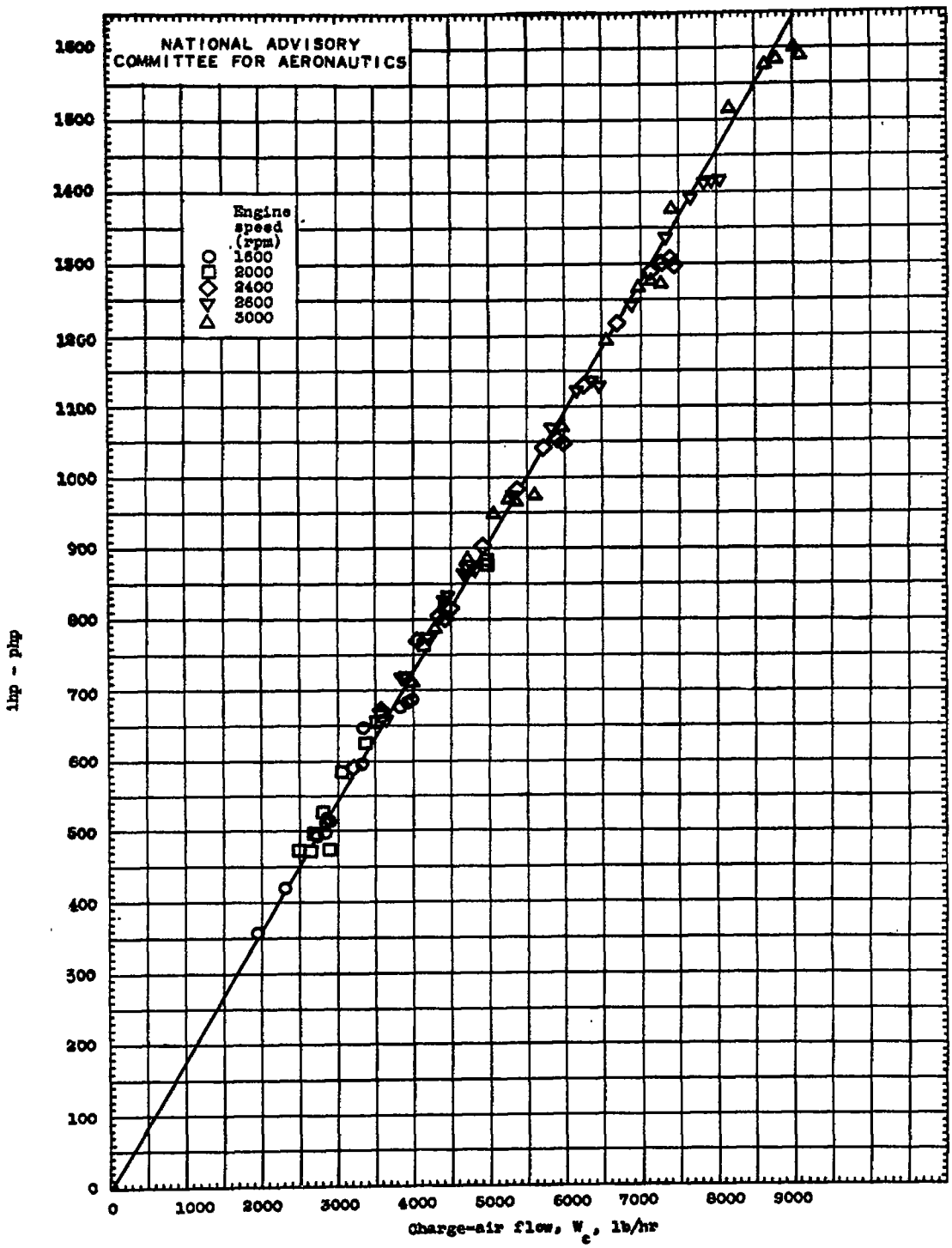

(b) Fuel-air ratio, 0.085.

Figure 9. - Continued. Variation of ihp - php with charge-air flow for various engine speeds and values of p_c/p_m. Values of ihp - php and charge-air flow W_c corrected to constant inlet-manifold mixture temperature T_m of 660° R.

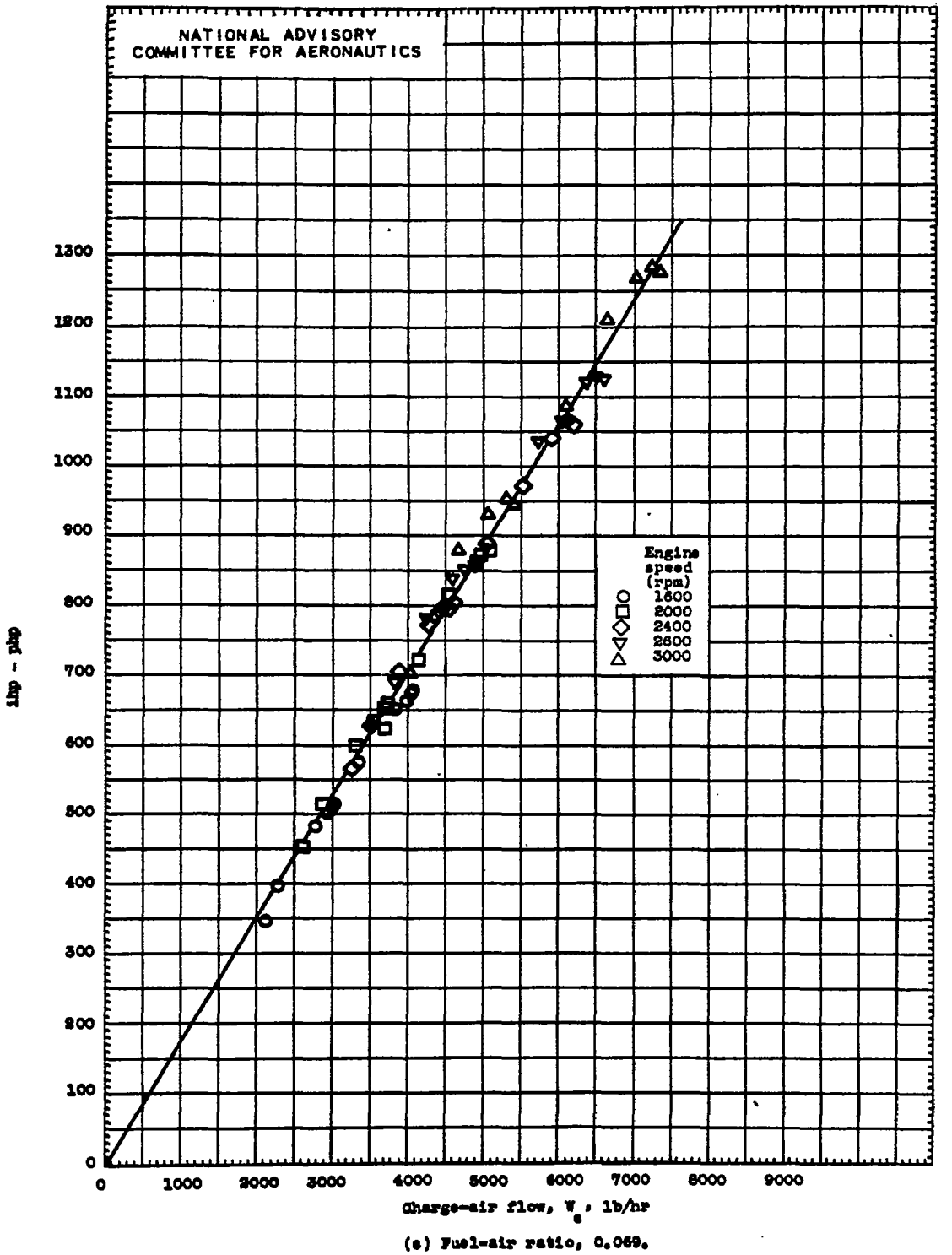

(a) Fuel-air ratio, 0.069.

Figure 9. - Continued. Variation of ihp - php with charge-air flow for various engine speeds and values of P_e/P_m. Values of ihp - php and charge-air flow W_c corrected to constant inlet-manifold mixture temperature T_m of 660° R.

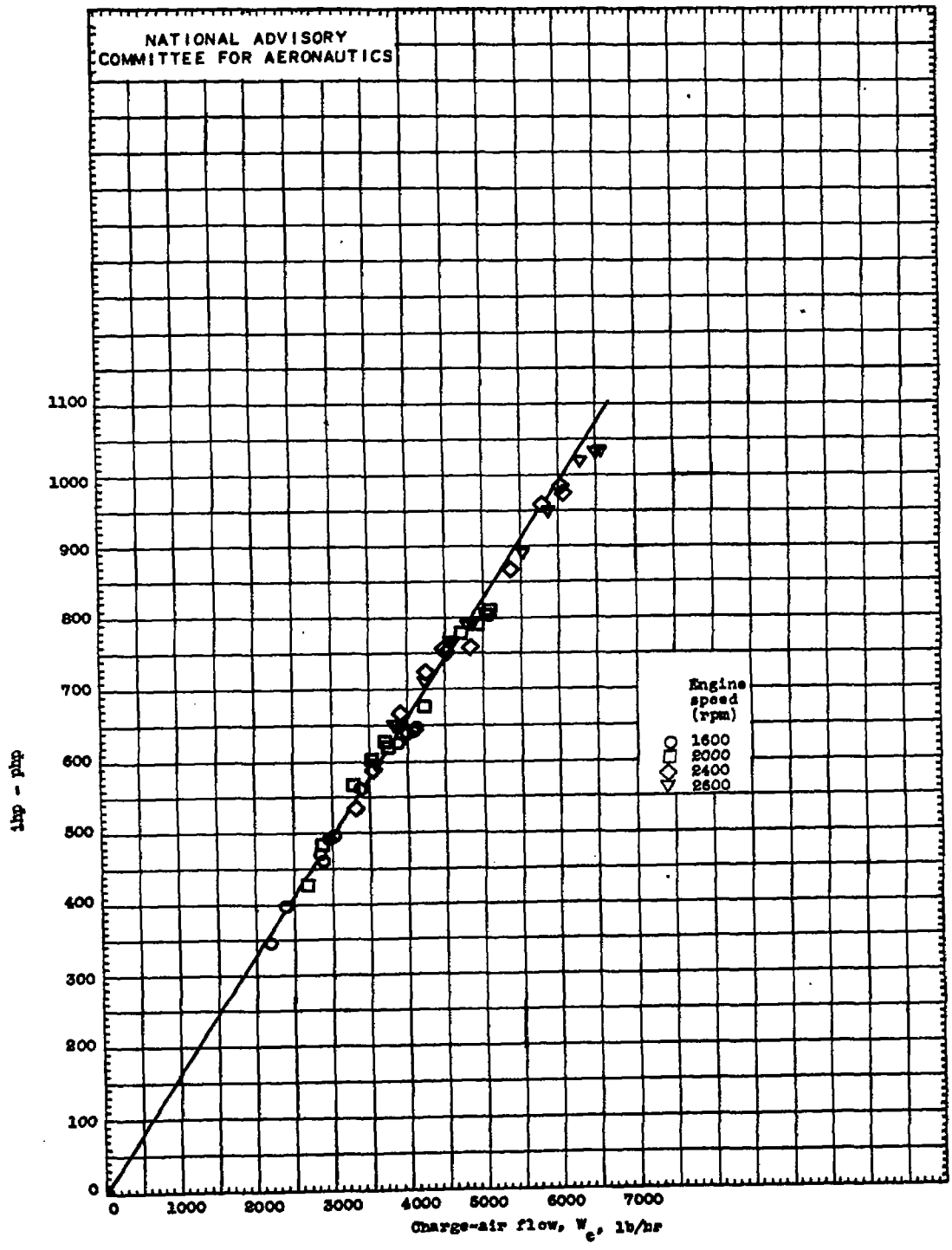

(d) Fuel-air ratio, 0.063.

Figure 9. - Concluded. Variation of ihp - php with charge-air flow for various engine speeds and values of p_e/p_m. Values of ihp - php and charge-air flow W_c corrected to constant inlet-manifold mixture temperature T_m of 660° R.

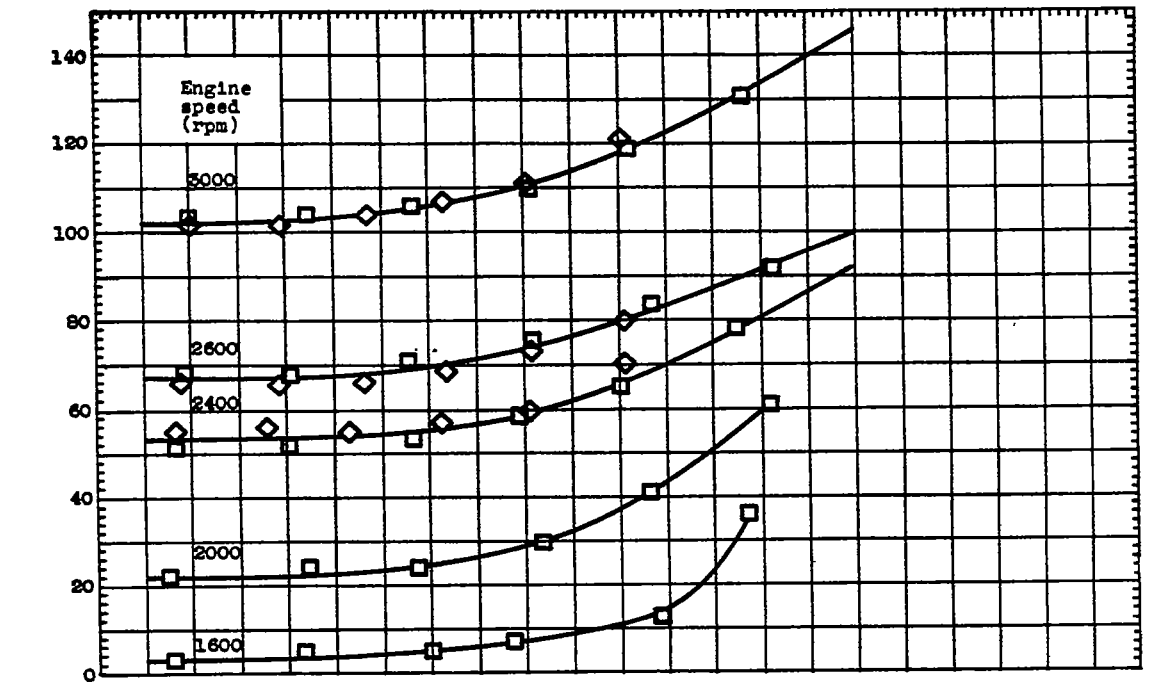

(a) Fuel-air ratio, 0.100.

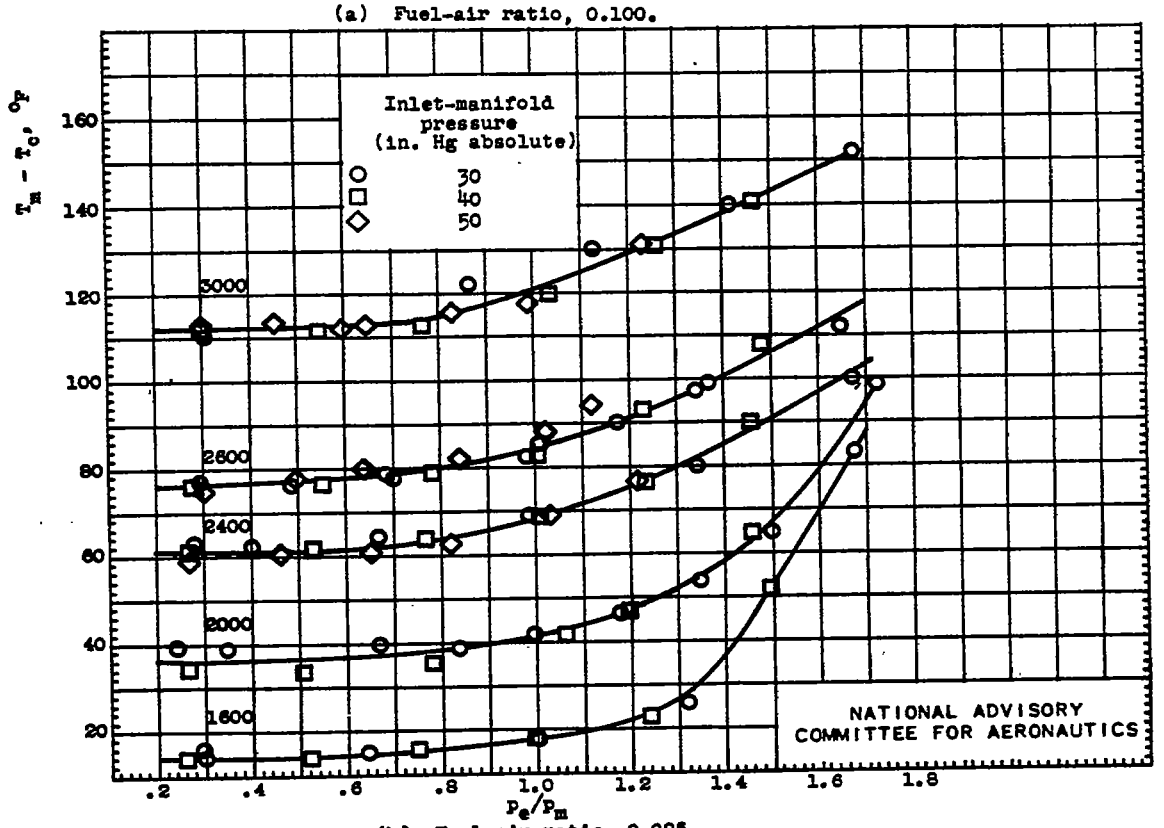

(b) Fuel-air ratio, 0.085.

Figure 10. - Variation of $T_m - T_c$ with P_e/P_m for constant engine speeds. Carburetor-air temperature T_c, 550° ± 15° R.

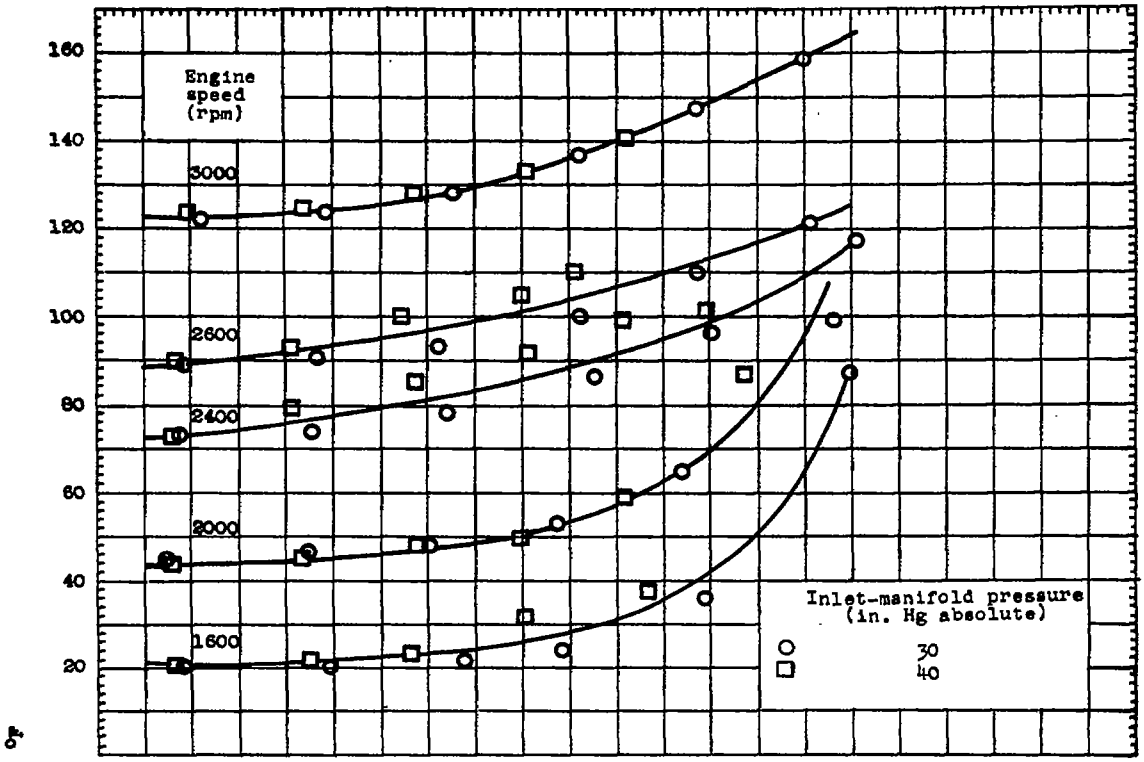

(c) Fuel-air ratio, 0.069.

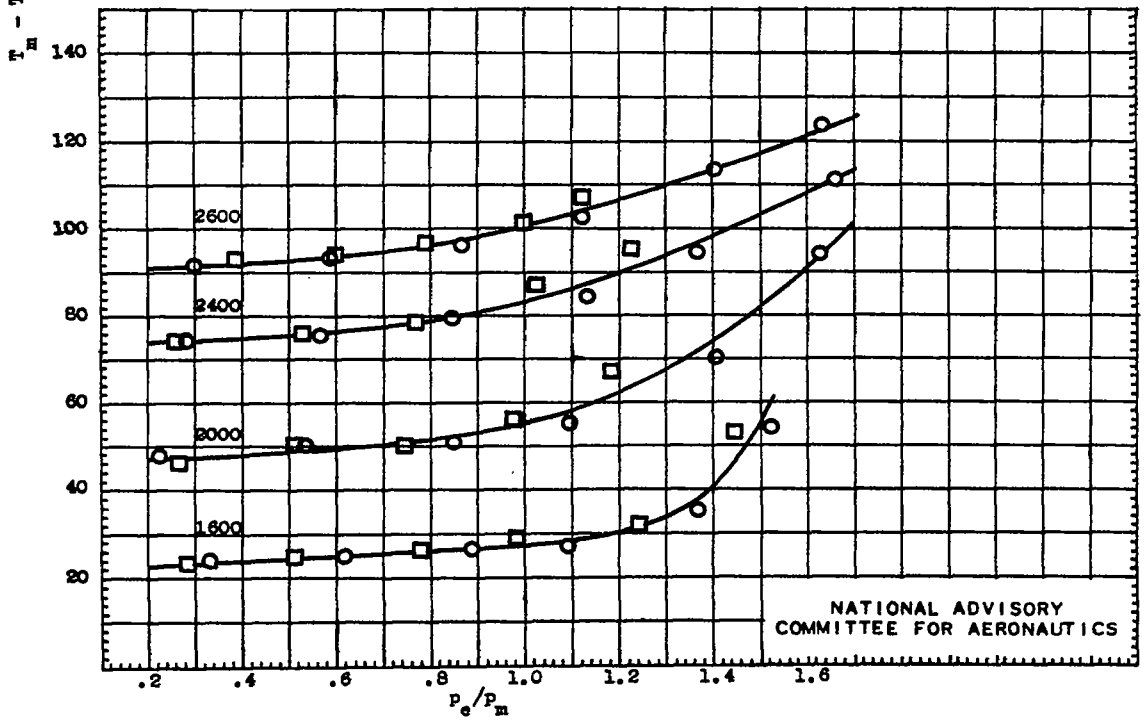

(d) Fuel-air ratio, 0.063.

Figure 10. - Concluded. Variation of $T_m - T_c$ with p_e/p_m for constant engine speeds. Carburetor-air temperature T_c, 550° ± 15° R.

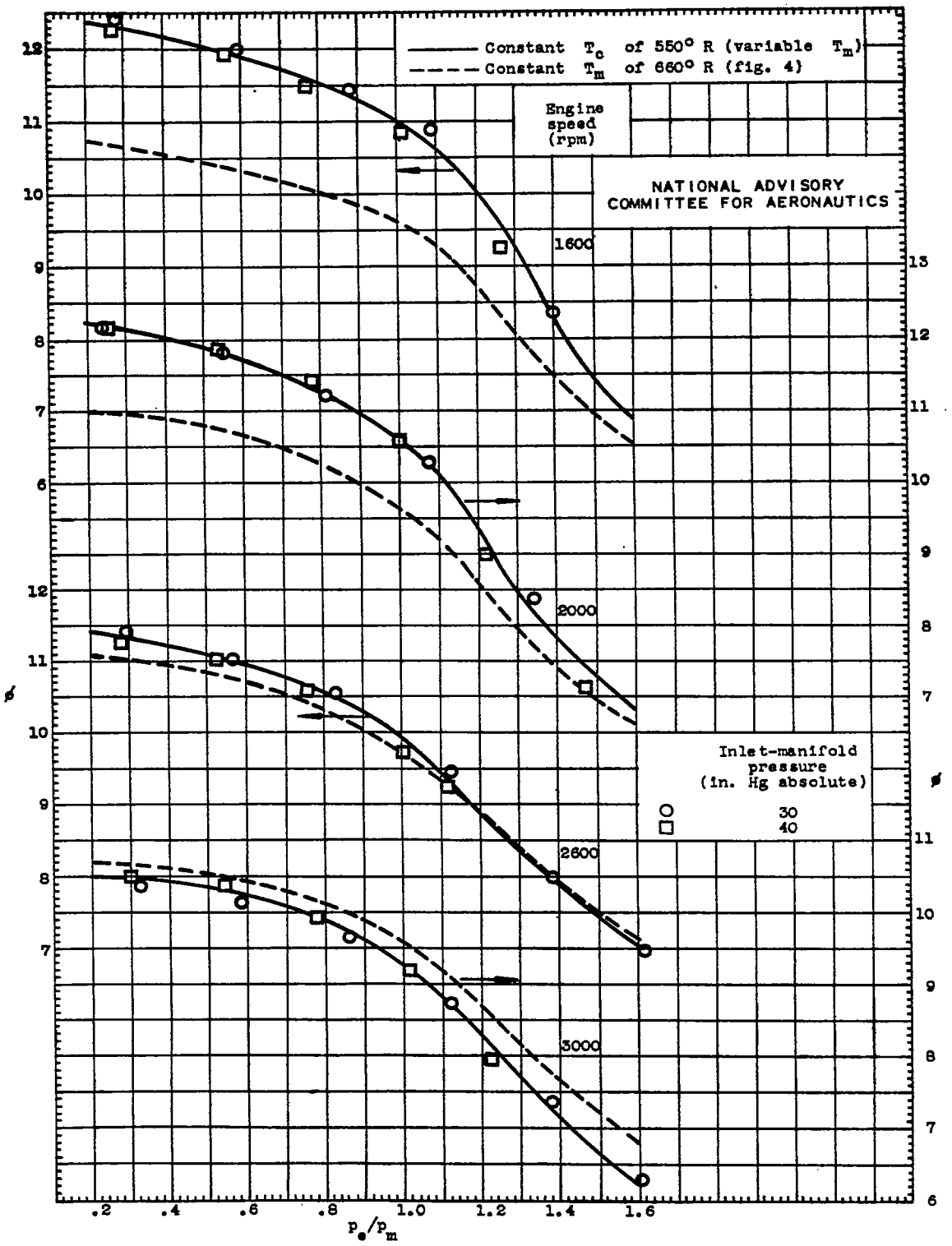

Figure 11. - Variation with p_e/p_m of ϕ corrected to constant inlet-manifold temperature as compared to that of ϕ corrected to constant carburetor-air temperature.

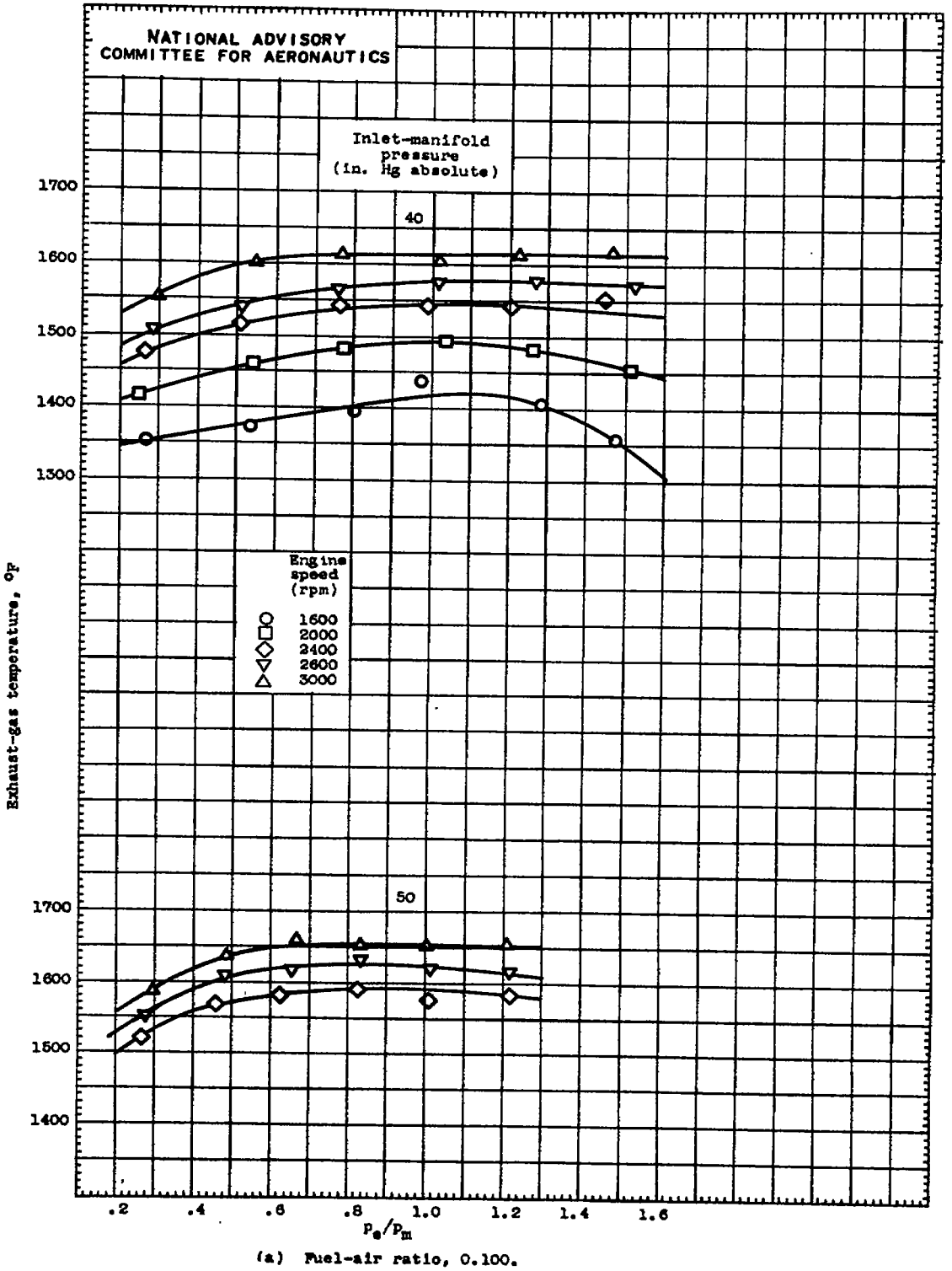

(a) Fuel-air ratio, 0.100.

Figure 12. - Variation of exhaust-gas temperature with p_e/p_m for constant engine speeds and inlet-manifold pressures.

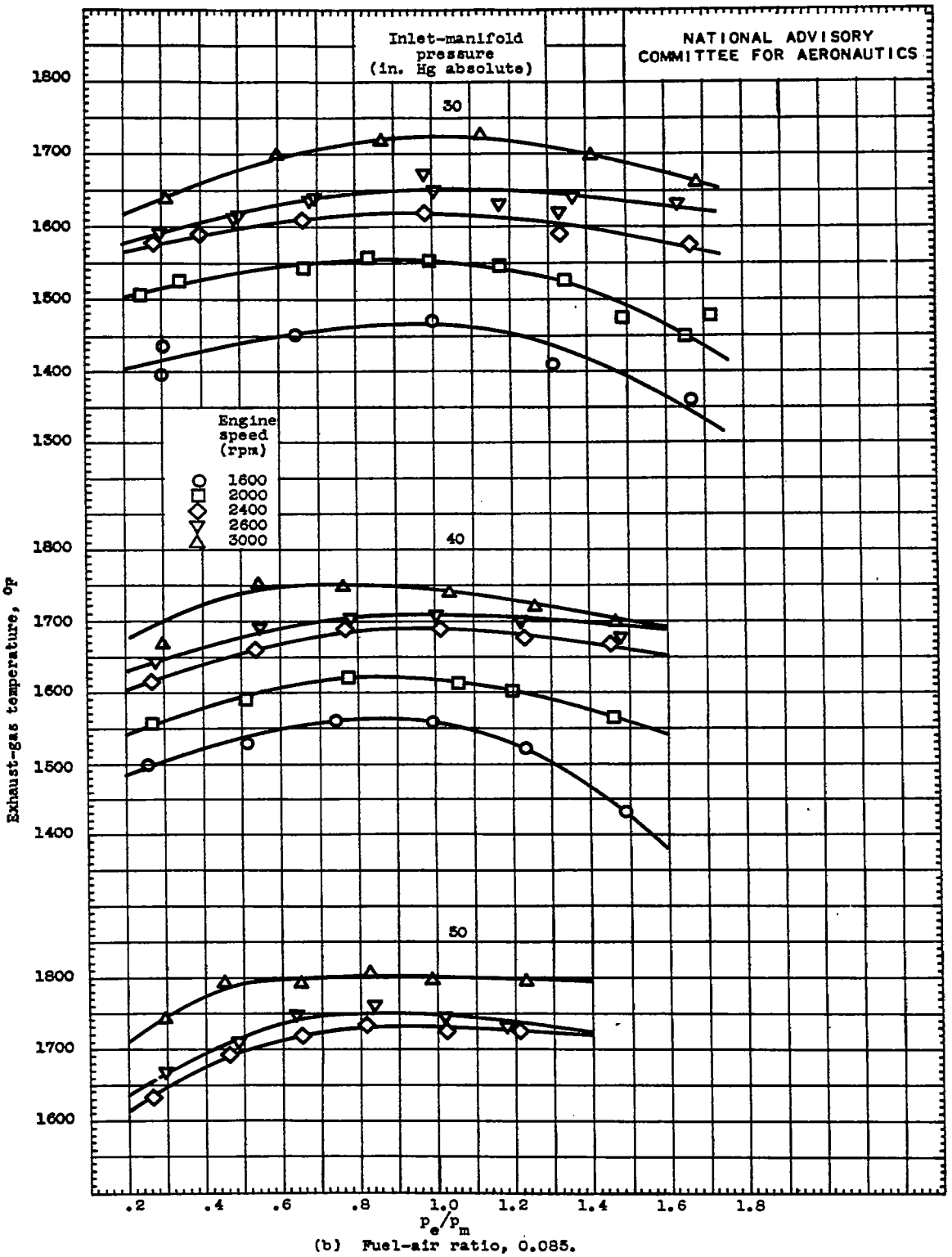

(b) Fuel-air ratio, 0.085.

Figure 12. - Continued. Variation of exhaust-gas temperature with p_e/p_m for constant engine speeds and inlet-manifold pressures.

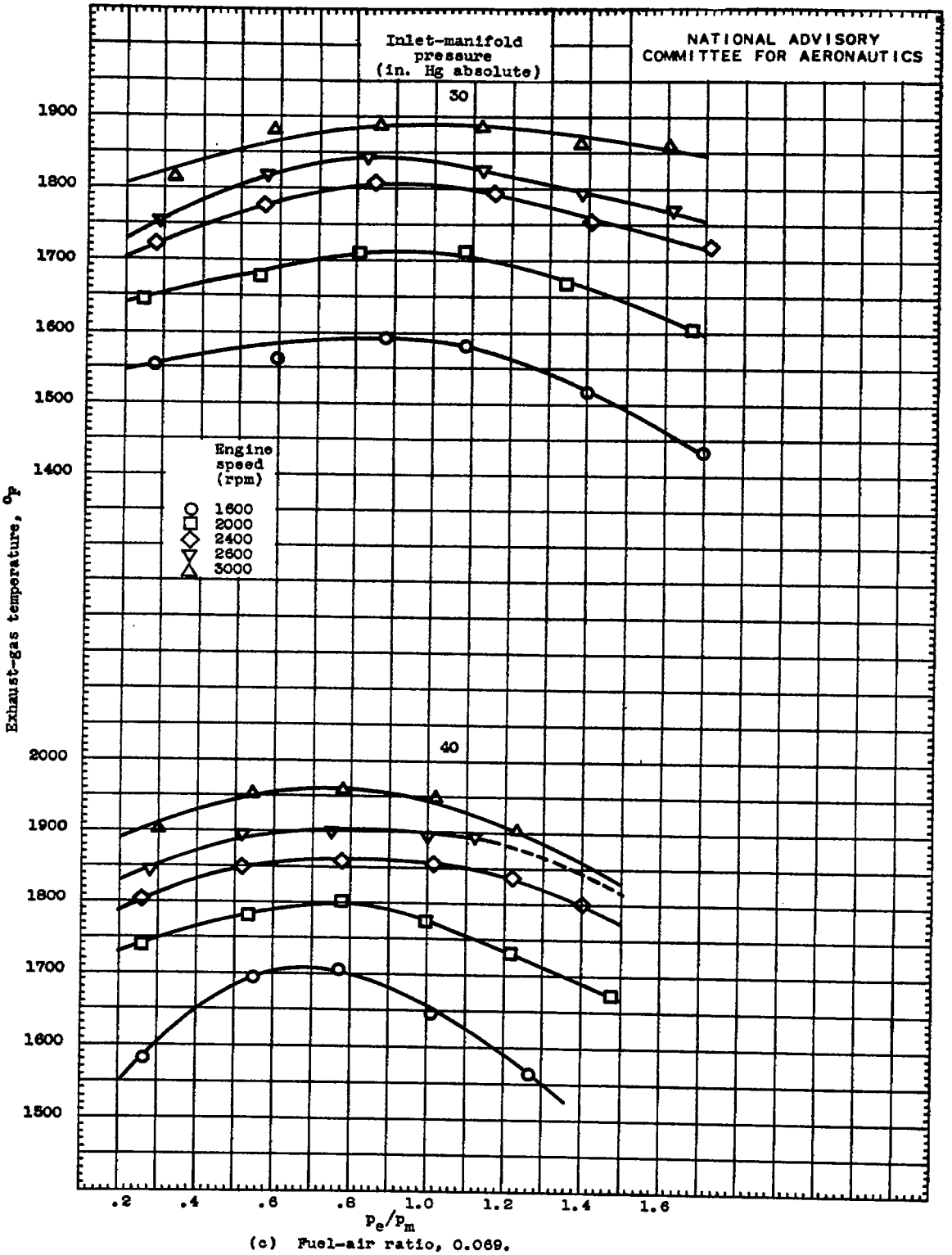

(c) Fuel-air ratio, 0.069.

Figure 12. - Continued. Variation of exhaust-gas temperature with p_e/p_m for constant engine speeds and inlet-manifold pressures.

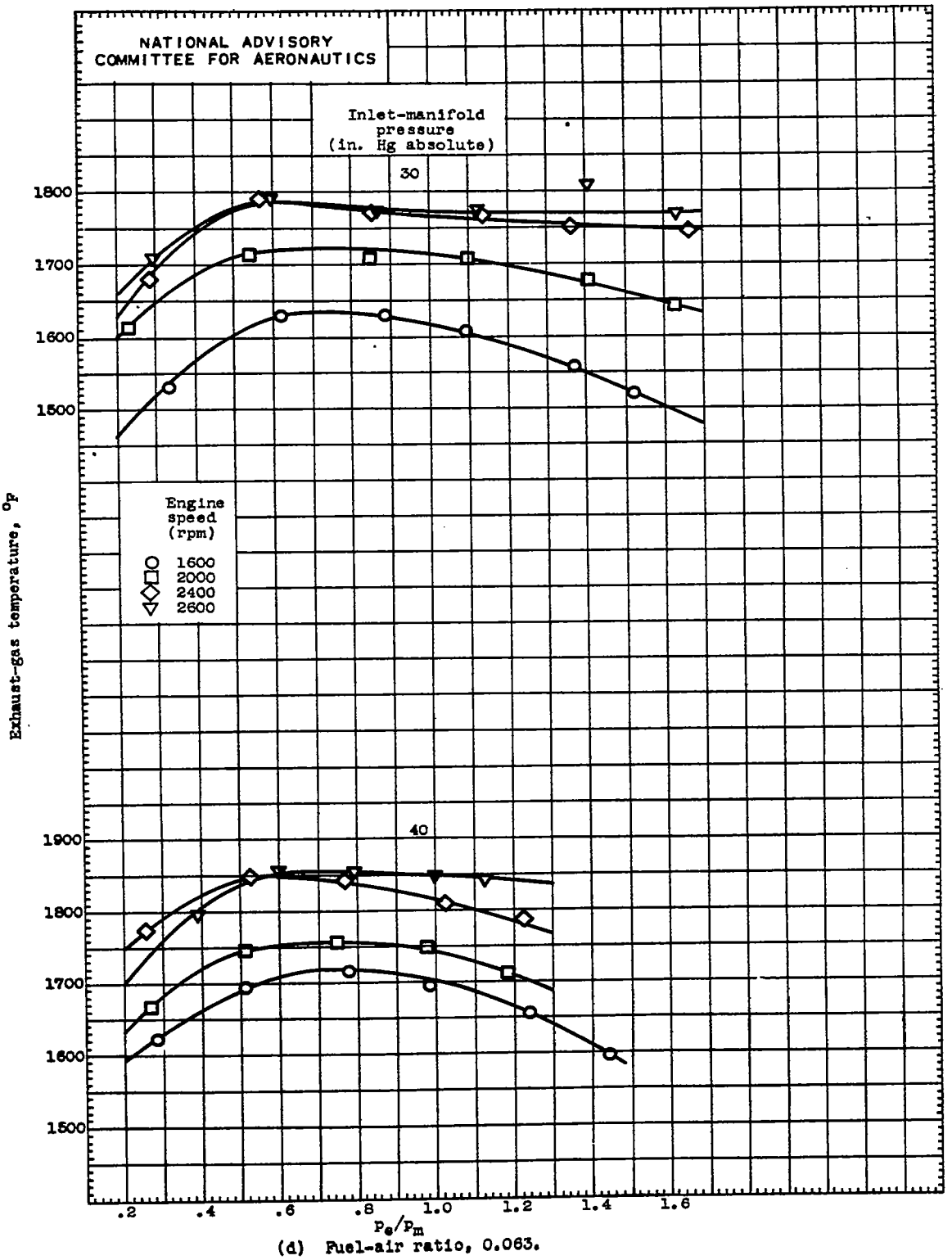

(d) Fuel-air ratio, 0.063.

Figure 12. - Concluded. Variation of exhaust-gas temperature with p_e/p_m for constant engine speeds and inlet-manifold pressures.

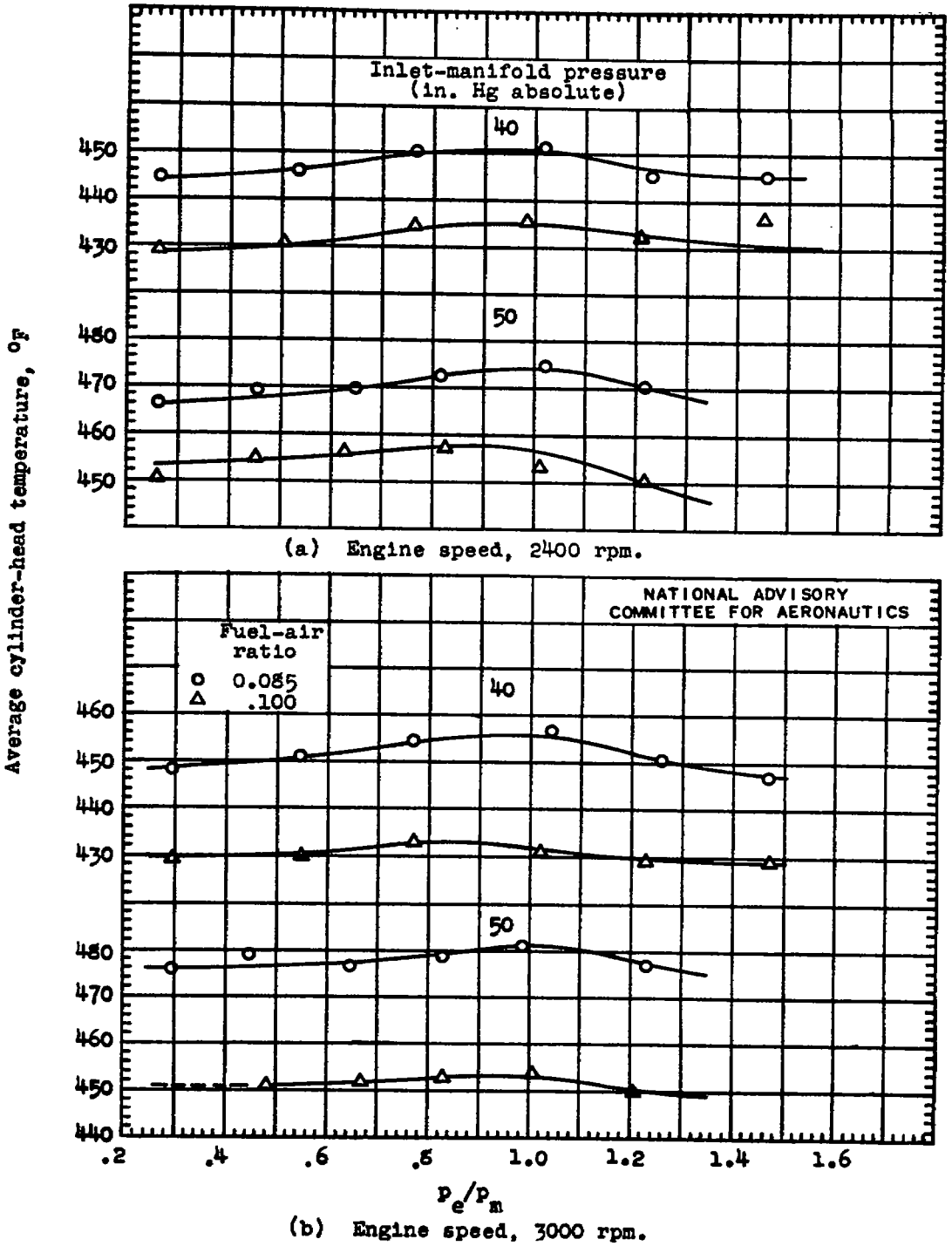

Figure 13. - Variation of average cylinder-head temperature between exhaust valves with p_e/p_m at fuel-air ratios of 0.100 and 0.085. Coolant, 70-30 ethylene glycol and water mixture; coolant flow, 0.71 pound per revolution; coolant outlet temperature, 220° ± 5° F.

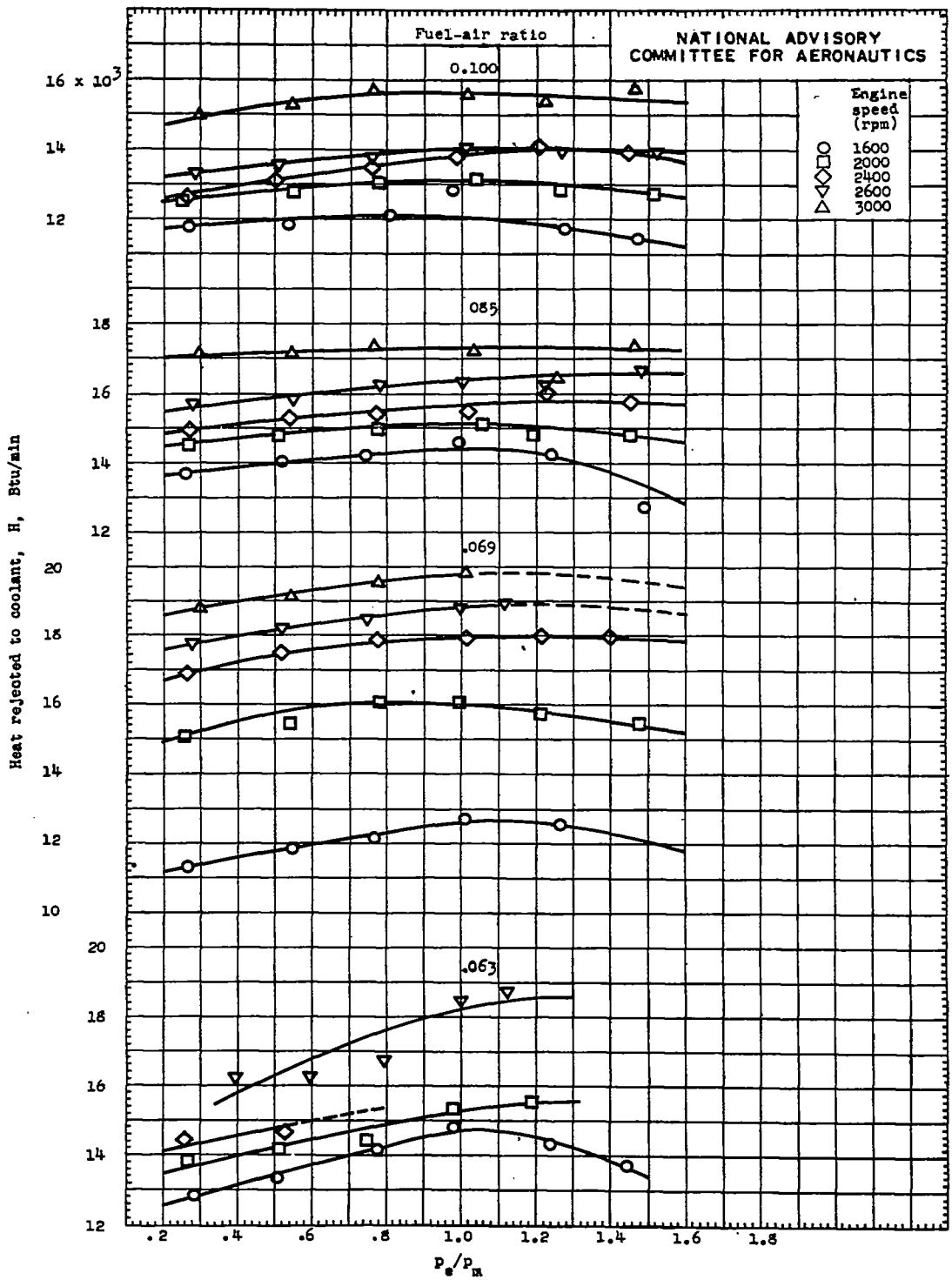

(a) Inlet-manifold pressure, 40 inches mercury absolute.

Figure 14. - Variation of heat rejected to coolant with p_e/p_m for constant engine speeds and fuel-air ratios. Coolant, 70-30 ethylene glycol and water mixture; coolant flow, 0.71 pound per revolution; coolant outlet temperature, 220° ± 5° F.

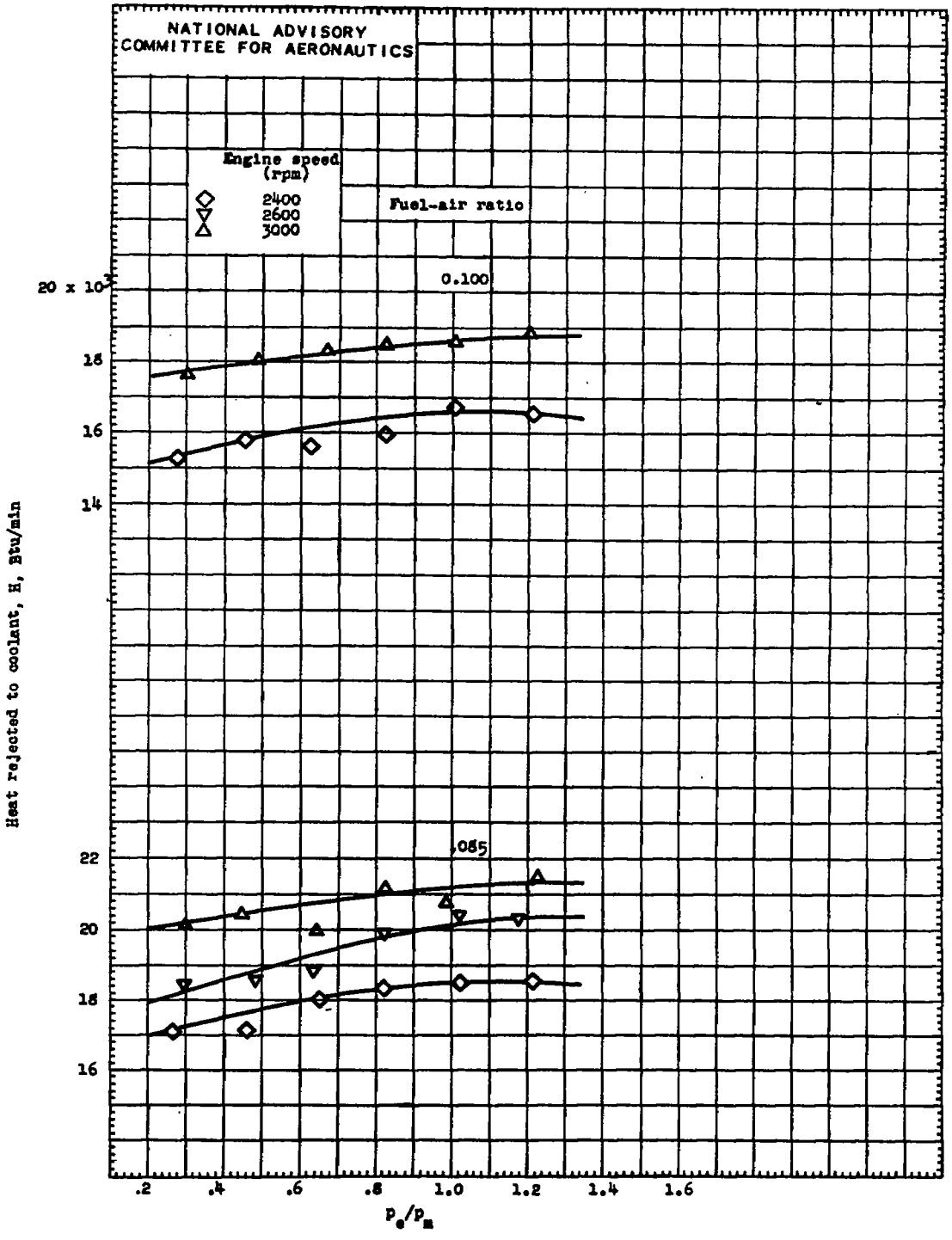

(b) Inlet-manifold pressure, 50 inches mercury absolute.

Figure 14. - Concluded. Variation of heat rejected to coolant with p_e/p_m for constant engine speeds and fuel-air ratios. Coolant, 70-30 ethylene glycol and water mixture; coolant flow, 0.71 pound per revolution; coolant outlet temperature, 220° ± 5° F.

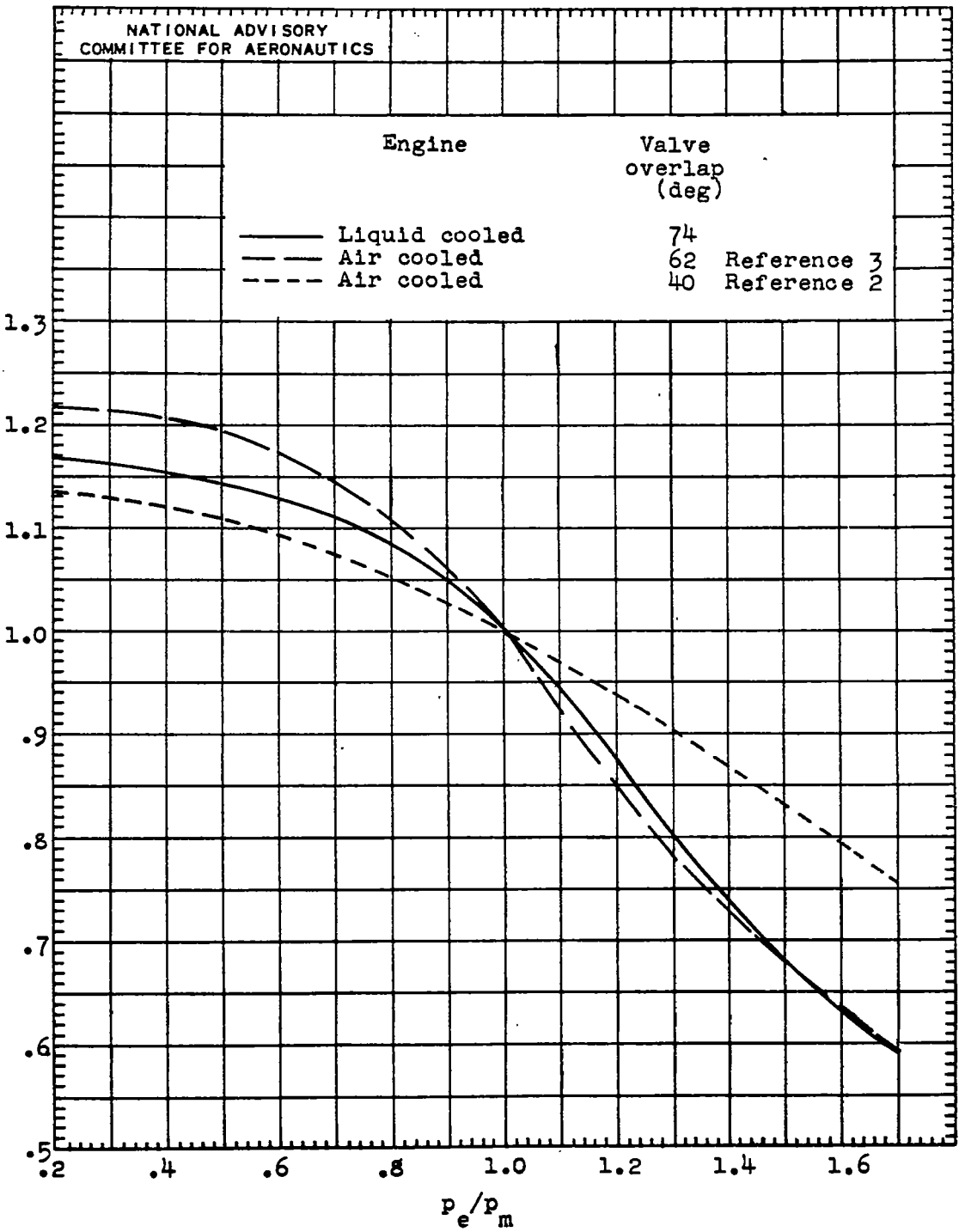

Figure 15. - Exhaust-pressure sensitivity of three engines operating at comparable conditions.